

AD-A051 852

CONNECTICUT UNIV STORRS DEPT OF MECHANICAL ENGINEERING  
PERTURBATION SOLUTIONS FOR VARIABLE ENERGY BLAST WAVES. (U)  
AUG 76 E T PITKIN

F/G 20/4

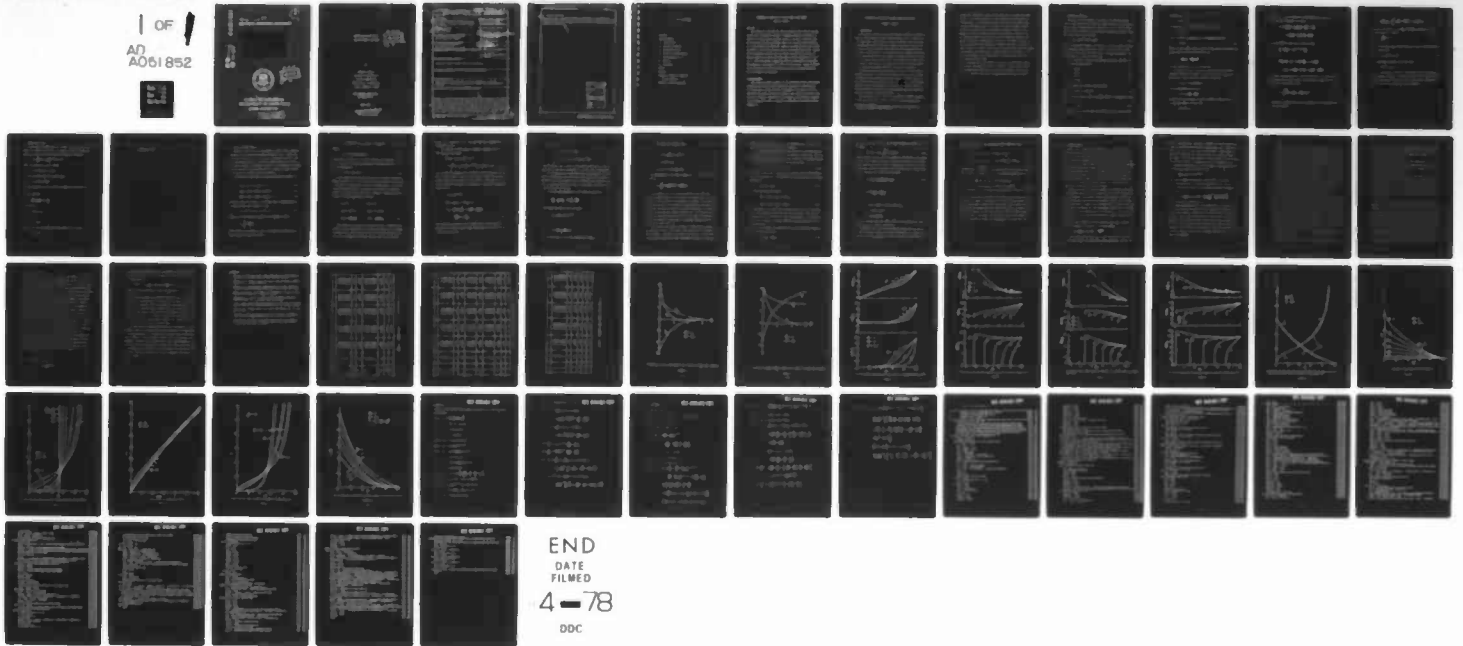
DAAG29-76-6-0142

UNCLASSIFIED

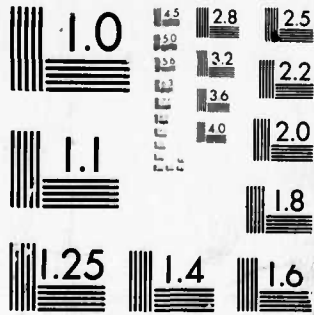
ARO-13483.2-E

NL

1 OF 1  
AD  
A051 852



0518

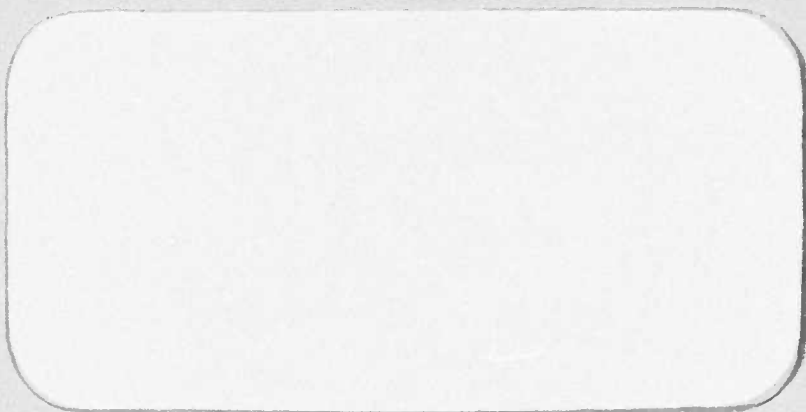


MICROCOPY RESOLUTION TEST CHART  
NATIONAL BUREAU OF STANDARDS-1963-A

AD A 051852

use → 410454  
MECHANICAL ENGINEERING DEPARTMENT

(8)  
SC



AD No. [ ]  
DDC FILE COPY



DDC  
MAR 28 1978  
F

~~SCHOOL OF ENGINEERING~~  
THE UNIVERSITY OF CONNECTICUT  
STORRS, CONNECTICUT

DISTRIBUTION STATEMENT A  
Approved for public release  
Distribution Unlimited

8

PERTURBATION SOLUTIONS FOR  
VARIABLE ENERGY BLAST WAVES

DDC  
MAR 28 1978  
F

by

Edward T. Pitkin  
Professor of Mechanical &  
Aerospace Engineering  
The University of Connecticut  
Storrs, Connecticut 06268

ARMY RESEARCH OFFICE GRANT  
DAAG 29-76-G0142  
E.K. Dabora, P. I.

August 1976

**DISTRIBUTION STATEMENT A**  
Approved for public release;  
Distribution Unlimited

18/ARO 19/3483.2-E

REPORT DOCUMENTATION PAGE

READ INSTRUCTIONS  
BEFORE COMPLETING FORM

1. REPORT NUMBER 13483.2-E ✓	2. JOVT ACCESSION NO.	3. RECIPIENT'S CATALOG NUMBER
4. TITLE (and Subtitle) Perturbation Solutions for Variable Energy Blast Waves	5. TYPE OF REPORT & PERIOD COVERED 9 Technical Report	6. PERFORMING ORG. REPORT NUMBER
7. AUTHOR(s) Edward T./Pitkin	8. CONTRACT OR GRANT NUMBER(s)	9. PROGRAM ELEMENT, PROJECT, TASK AREA & WORK UNIT NUMBERS 15 DAAG29-76-G-0142 DA-ARO-D-31-224-78-G100
9. PERFORMING ORGANIZATION NAME AND ADDRESS The University of Connecticut Storrs, Connecticut 06268	10. PROGRAM ELEMENT, PROJECT, TASK AREA & WORK UNIT NUMBERS 12 59p.	11. REPORT DATE August 1976
11. CONTROLLING OFFICE NAME AND ADDRESS U. S. Army Research Office Post Office Box 12211 Research Triangle Park, NC 27709	12. REPORT DATE	13. NUMBER OF PAGES 53
14. MONITORING AGENCY NAME & ADDRESS (if different from Controlling Office)	15. SECURITY CLASS. (of this report) Unclassified	15a. DECLASSIFICATION/DOWNGRADING SCHEDULE

16. DISTRIBUTION STATEMENT (of this Report)  
Approved for public release; distribution unlimited.

17. DISTRIBUTION STATEMENT (of the abstract entered in Block 20, if different from Report)

18. SUPPLEMENTARY NOTES  
The findings in this report are not to be construed as an official Department of the Army position, unless so designated by other authorized documents.

19. KEY WORDS (Continue on reverse side if necessary and identify by block number)

20. ABSTRACT (Continue on reverse side if necessary and identify by block number) The trajectory of and the flow field behind blast waves with time varying energy input is determined. Freeman's Lagrangean coordinate formulation is modified to include both the geometric factor,  $\alpha$ , for plane, cylindrical and spherical shocks and also non-integer values of  $\beta$ , the energy input parameter, in a single computational algorithm. Numerical problems associated with vanishing density at the fictitious piston face are then examined and solved. Second order perturbation solutions about the infinite strength shock are then obtained in Sakurai's inverse shock Mach number expansion parameter for  $0 < \beta < \alpha + 1$ .  
Cor =

beta  
next page  
alpha

20. ABSTRACT CONTINUED

Tables and graphs of significant numerical coefficients are presented for comparison to and extension of results of other authors. Graphs of typical shock trajectories and flow field density, pressure and velocity variations are also presented and discussed.



ACCESSION for	
NTIS	White Section <input checked="" type="checkbox"/>
DDC	Buff Section <input type="checkbox"/>
UNANNOUNCED	<input type="checkbox"/>
JUSTIFICATION _____	
BY _____	
DISTRIBUTION/AVAILABILITY CODES	
Disc. _____/or SPECIAL	
A	

TABLE OF CONTENTS

ABSTRACT	i
ACKNOWLEDGEMENTS	i
1. INTRODUCTION	1
2. EQUATIONS OF MOTION	3
3. STRONG SHOCK LIMIT	7
4. OUTLINE OF SERIES SOLUTION	9
5. EXTRAPOLATION TO $m = 0$	17
6. RESULTS	19
7. REFERENCES	23
TABLES	24
FIGURES	27
APPENDIX A, SUMMARY OF EQUATIONS FOR COMPUTATION	A-1
APPENDIX B, COMPUTER PROGRAMS	B-1

## PERTURBATION SOLUTIONS FOR VARIABLE ENERGY BLAST WAVES

Edward T. Pitkin

### ABSTRACT

The trajectory of and the flow field behind blast waves with time varying energy input is determined. Freeman's<sup>2</sup> Lagrangean coordinate formulation is modified to include both the geometric factor,  $\alpha$ , for plane, cylindrical and spherical shocks and also non-integer values of  $\beta$ , the energy input parameter, in a single computational algorithm. Numerical problems associated with vanishing density at the fictitious piston face are then examined and solved. Second order perturbation solutions about the infinite strength shock are then obtained in Sakurai's<sup>1</sup> inverse shock Mach number expansion parameter for  $0 \leq \beta < \alpha + 1$ . Tables and graphs of significant numerical coefficients are presented for comparison to and extension of results of other authors. Graphs of typical shock trajectories and flow field density, pressure and velocity variations are also presented and discussed.

### ACKNOWLEDGEMENTS

This work was partially supported by the Army Research Office under Grants DA-ARO-D-31-124-73-G100 and DAAG 29-76-G0142. The author is most grateful to Professor Eli K. Dabora, principal investigator of both grants, who first suggested this problem and willingly engaged in many fruitful discussions along the road to solution. Computations were performed at The University of Connecticut Computer Center which is supported by Grant GJ-9 of the National Science Foundation.



## PERTURBATION SOLUTIONS FOR VARIABLE ENERGY BLAST WAVES

Edward T. Pitkint

### 1. INTRODUCTION

The analytical theory of blast waves has been the subject of intensive study by many investigators since the pioneering work of G. I. Taylor<sup>5</sup> about thirty years ago. A large fraction of this work concerns waves of constant, instantaneously supplied energy which propagate and decay according to the dictates of inviscid isentropic flow behind the wave and Rankine-Hugoniot conditions at the wave front. This work has been well summarized by Sakurai<sup>1</sup> who has also developed an efficient method of expanding the general solution about the simpler limiting solution for the flow behind a very strong shock. Furthermore, he has shown that the square of the inverse shock Mach number is a most convenient and natural parameter to use for this expansion.

A lesser amount of work has been devoted to analysis of blast waves of variable energy input. In 1957 Lees and Kubota<sup>6</sup> examined this case briefly in connection with the hypersonic blast wave analogy and Rogers<sup>3</sup> presented the limiting strong shock solution in 1958. More recently in 1968 Freeman<sup>2</sup> examined this case in connection with cylindrical spark channel formation from exploding wires and Dabora<sup>7</sup> has applied variable blast wave techniques to droplet explosions in spray detonations.

The work reported here is basically an extension of Freeman's approach to cover the full spectrum of plane, cylindrical and spherical variable

---

† Professor of Mechanical and Aerospace Engineering, The University of Connecticut, Storrs, Connecticut 06268

energy blast waves within a single analytic formulation and computation algorithm. It also contains corrections to some numerical errors discovered in Freeman's paper. As a consequence Freeman's notation has been adopted completely and derivations given in his paper have only been summarized here. His major contribution was to recast Sakurai's expansion procedure in Lagrangean coordinates, replacing distance from the origin,  $r$ , with mass,  $m$ , as an independent variable, but retaining the inverse shock Mach number as the expansion parameter. The advantage is two fold: (1) the number of differential equations that must ultimately be integrated numerically is reduced by nearly a factor of two, and (2) the position of the fictitious moving piston face which supplies the variable energy is uniquely defined to be at  $mass = 0$ . In Eulerian coordinates precise determination of the piston position can be a very difficult numerical task.

In sections 2 and 3, the equations of motion and the strong shock solution are reviewed. The expansion procedure is outlined in section 4 and a method of extrapolating the numerical solution to the mass origin is discussed in section 5. Numerical results are then summarized and discussed in section 6.

## 2. EQUATIONS OF MOTION

Let  $p_0$  and  $\rho_0$  be the pressure and density in the undisturbed medium while  $r$  is the radius from the origin to an arbitrary point in space and  $M$  is the total mass contained between the origin and  $r$ . Let  $r = R$  at the shock front so that the volume behind the shock front, when filled with gas of original density, will contain the mass

$$M_0 = 2^\alpha \pi^{\alpha(3-\alpha)/2} R^{\alpha+1} \rho_0 / (\alpha+1) \quad (2.1)$$

where  $\alpha$  is a geometric parameter with values 0, 1, and 2 for plane, cylindrical and spherical waves respectively. Finally let  $u$  be the speed at any point and  $U$  be the speed of the shock front,  $C$  the speed of sound and  $\gamma$  the specific heat ratio in the undisturbed gas.

It is convenient to introduce non-dimensional variables. For mass, radius, velocity and density take

$$m \triangleq M/M_0 \quad (2.2)$$

$$a \triangleq r/R \quad (2.3)$$

$$f \triangleq u/U \quad (2.4)$$

$$h \triangleq \rho/\rho_0 \quad (2.5)$$

while the square of the inverse shock Mach number

$$y \triangleq c^2/U^2 = c^2/(dR/dt)^2 \quad (2.6)$$

may be combined with  $p_0$  to define a variable related to non-dimensional pressure

$$g = py/p_0 \quad (2.7)$$

An arbitrary non-zero initial radius of the shock,  $R_0$ , is then used to define

a characteristic time

$$t_0 \triangleq R_0/C \quad (2.8)$$

which may then be used to non-dimensionalize time through

$$\omega \triangleq t/t_0 \quad (2.9)$$

while the shock front coordinate, R, is non-dimensionalized by

$$z \triangleq R/R_0 \quad (2.10)$$

Finally the decay index, a ratio of the percentage changes of shock Mach number and radius, as introduced by Sakurai<sup>1</sup>, is

$$\lambda = \frac{(dy/y)}{(dz/z)} = \frac{-2Rd^2R/dt^2}{(dR/dt)^2}, \quad (2.11)$$

the latter obtained by use of (2.6) and (2.10).

The equations of fluid flow behind the shock wave have been derived in Lagrangean coordinates by Freeman<sup>2</sup>. Only the results will therefore be summarized here. First the density at any point is given by

$$h = \rho/\rho_0 = 1/[(\alpha+1)a^\alpha \partial a/\partial m] \quad (2.12)$$

and the non-dimensional velocity is

$$f = a - (\alpha+1)m \frac{\partial a}{\partial m} + \lambda y \frac{\partial a}{\partial y}. \quad (2.13)$$

Beginning with the assumption of a purely isentropic process behind the shock for each mass element it follows that

$$\partial(p/\rho^\gamma)/\partial y = 0 \quad (2.14)$$

which upon using the non-dimensional variables above can be shown to lead to the following in Lagrangean coordinates,

$$\begin{aligned}
 (\alpha+1)m \left[ \left( \frac{\alpha}{a} \frac{\partial a}{\partial m} + \frac{1}{\gamma g} \frac{\partial g}{\partial m} \right) \frac{\partial a}{\partial m} + \frac{\partial^2 a}{\partial m^2} \right] + \frac{\lambda}{\gamma} \frac{\partial a}{\partial m} \\
 - \lambda y \left[ \left( \frac{\alpha}{a} \frac{\partial a}{\partial y} + \frac{1}{\gamma g} \frac{\partial g}{\partial y} \right) \frac{\partial a}{\partial m} + \frac{\partial^2 a}{\partial m \partial y} \right] = 0 .
 \end{aligned} \tag{2.15}$$

Similarly Newton's second law for the mass element

$$\frac{\partial u}{\partial t} = \frac{\partial u}{\partial y} \frac{dy}{dt} = -(2r)^\alpha \pi^{\alpha} a^{(3-\alpha)/2} \frac{\partial p}{\partial m} \tag{2.16}$$

lead: to

$$\begin{aligned}
 \frac{a^\alpha (\alpha+1)}{\gamma} \frac{\partial g}{\partial m} - \frac{\lambda a}{2} + (\alpha+1) \frac{2\alpha+\lambda}{2} m \frac{\partial a}{\partial m} + (\alpha+1)^2 m^2 \frac{\partial^2 a}{\partial m^2} \\
 + \lambda y \left[ -2(\alpha+1)m \frac{\partial^2 a}{\partial m \partial y} + \frac{2+\lambda}{2} \frac{\partial a}{\partial y} + y \frac{\partial a}{\partial y} \frac{\partial \lambda}{\partial y} + \lambda y \frac{\partial^2 a}{\partial y^2} \right] = 0 .
 \end{aligned} \tag{2.17}$$

The energy contained between the origin and the shock is the sum of the kinetic energy and the internal energy. The increment of energy over that of the same volume of undisturbed gas is

$$E = \int_0^{M_0} \left( \frac{u^2}{2} + \frac{p}{(\gamma-1)\rho} - \frac{p_0}{(\gamma-1)\rho_0} \right) dm . \tag{2.18}$$

Converting to non-dimensional form, using Equation (2.12) and letting a prime designate  $\partial/\partial m$  gives

$$\frac{E_{p_0}}{(\alpha+1)p_0 M_0} = \frac{1}{y} \int_0^1 \left( \frac{\gamma r^2}{2(\alpha+1)} + \frac{g a^\alpha a'}{\gamma-1} \right) dm - \frac{1}{(\gamma-1)(\alpha+1)} \quad (2.19)$$

Letting  $b = 1/[(\gamma-1)(\alpha+1)]$ ,  $E_\alpha = E/[2\pi^{(3-\alpha)/2}]^\alpha$  and designating the integral  $J$  after Sakurai<sup>1</sup> this becomes

$$\frac{E_\alpha}{p_0 R^{\alpha+1}} = \frac{J}{y} - b \quad (2.20)$$

If the total energy behind the shock varies as a power of time according to the following rule

$$E_\alpha = R_0^{\alpha+1} p_0 (t/t_0)^\beta, \quad (2.21)$$

the energy equation reduces to the simple form

$$\omega^\beta / z^{\alpha+1} = J/y - b. \quad (2.22)$$

When  $\beta = 0$  the energy is constant, a case examined by many investigators and well documented by Sakurai. Letting  $\beta$  take non-zero values allows one to model a fairly wide range of energy inputs which can be further extended with some modification of (2.21) as has been shown by Freeman<sup>2</sup>.

### 3. STRONG SHOCK LIMIT

At very large shock Mach numbers  $y \rightarrow 0$  and  $J/y \gg b$  so the energy equation reduces to a simple form consistent with Rogers'<sup>3</sup> similarity solution for the equation of motion for which the shock front advances according to

$$R = \left[ R_0^{\alpha+1} C^2 / n^2 J_0 t_0^\beta \right]^{1/(\alpha+3)} t^n = K t^n \quad (3.1)$$

where  $n$  is related to  $\beta$ ,  $\alpha$  and  $\lambda$  through

$$n = (2+\beta)/(\alpha+3) = 2/(\lambda_0+2) \quad (3.2)$$

from which the decay index for strong shocks is

$$\lambda_0 = 2(\alpha+1-\beta)/(2+\beta) \quad (3.3)$$

The zero subscripts on  $\lambda$  and  $J$  are used to designate the strong shock case here.

Note also that

$$\frac{dz}{d\omega} = \frac{t_0}{R_0} \frac{dR}{dt} = \frac{U}{C} = \frac{1}{y^{1/2}} \quad (3.4)$$

while from (3.1)

$$dz/d\omega = nz/\omega \quad (3.5)$$

so that

$$z = \omega / n y^{1/2} \quad (3.6)$$

Combining this with the strong shock energy equation ( $b = 0$ ) yields

$$z = z_0 y^{1/\lambda_0} \quad (3.7)$$

where

$$z_0 = \left( n^\beta / J_0 \right)^{1/(\alpha+1-\beta)} \quad (3.8)$$



#### 4. OUTLINE OF SERIES SOLUTION

Equations (2.15) (2.17) and (2.22) comprise a system of three dependent variables;  $\lambda$ ,  $a$ , and  $g$  and two independent variables;  $m$  and  $y$ . Sakurai has shown that  $\lambda$  is a function of  $y$  only and that the pressure, density etc. are slowly varying functions of  $y$ . He therefore suggests expansion in powers of  $y$  to reduce the number of independent variables. In the Lagrangean coordinates used here this has the very desirable effect of reducing the partial differential equations to ordinary differential equations.

The expansions, taken about the strong shock solution for which  $y = 0$ , are

$$\lambda(y) = \lambda_0 + \lambda_1 y + \lambda_2 y^2 + \dots \quad (4.1)$$

$$a(m,y) = a_0(m) + a_1(m)y + a_2(m)y^2 + \dots \quad (4.2)$$

$$g(m,y) = g_0(m) + g_1(m)y + g_2(m)y^2 + \dots \quad (4.3)$$

By similar reasoning the equation for the shock front is expanded about the strong shock "zero order" solution (3.7) as

$$z = z_0 y^{1/\lambda_0} (1 + z_1 y + z_2 y^2 + \dots) \quad (4.4)$$

Equation (3.4) which applies in general can be integrated to give:

$$\omega = \int y^{1/2} \frac{dz}{dy} dy \quad .$$

Substituting for  $z$  and taking  $z = 0$  at  $\omega = 0$  then gives an expansion for the time variable as a function of  $y$  and  $z$

$$\omega = z_0 y^{(\lambda_0+2)/2\lambda_0} (\omega_0 + \omega_1 z_1 y + \dots + \omega_j z_j y^j + \dots) \quad (4.6)$$

where

$$\omega_j = (2j\lambda_0+2)/((2j+1)\lambda_0+2) \quad (4.7)$$

Noting from (2.13) that  $f = f(\lambda, a, m)$  it is clear that substitution of (4.1 - 4.3) into (2.19) will yield integrals in ascending powers of  $y$  so that  $J$  can be expressed as

$$J = J_0 + J_1 y + J_2 y^2 + \dots \quad (4.8)$$

These expansions are then substituted into the isentropic, momentum and energy equations (2.15), (2.17) and (2.22) and the coefficients of like powers of  $y$  equated to give perturbation equations of ascending order. In the isentropic and momentum equations this procedure yields ordinary differential equations for  $a_j$  and  $g_j$  with  $\lambda_j$  entering as a parameter. These must be solved subject to the shock jump boundary conditions.

$$\begin{aligned} a_0(1) &= 1 & a_1(1) &= 0 \\ g_0(1) &= 2\gamma/(\gamma+1) & g_1(1) &= (1-\gamma)/(\gamma+1) \\ a'_0(1) &= \frac{\gamma-1}{(\alpha+1)(\gamma+1)} & a'_1(1) &= \frac{2}{(\alpha+1)(\gamma+1)} \end{aligned} \quad (4.9)$$

The remaining coefficients are all zero at the shock. Fortunately the successive orders of approximation to the isentropic equation yield intermediate integrals for  $g_j$ . These may then be used in the momentum equation which must be solved by numerical integration from the shock front to the mass

origin. The equations and solutions for each order will be discussed in the following sections.

Now consider the energy equation. Putting the expansion (4.4), (4.6) and (4.8) into (2.22) gives

$$z_0^\beta (\omega_0 + \omega_1 z_1 y + \omega_2 z_2 y^2 + \dots)^\beta = z_0^{\alpha+1} (1 + z_1 y + z_2 y^2 + \dots)^{\alpha+1} (J_0 + (J_1 - b)y + J_2 y^2 + \dots). \quad (4.10)$$

The two series with exponents may be converted to simple power series by means of the binomial formula if the first term of each is larger than the sum of the remaining terms. This is certainly true for small  $y$ . Multiplying out on the right and equating coefficients of like powers of  $y$  then yields relations between  $J_j$  and  $z_j$ :

$$J_0 = \omega_0^\beta z_0^{\beta - (\alpha+1)},$$

$$J_1/J_0 = \left[ \beta \omega_1 / \omega_0 - (\alpha+1) \right] z_1 + b,$$

$$J_2/J_0 = \left[ \beta \frac{(\beta-1)}{2} \frac{\omega_1^2}{\omega_0^2} + (\alpha+1) \left( \frac{\alpha+2}{2} - \frac{\beta \omega_1}{\omega_0} \right) \right] z_1^2 + \left[ \frac{\beta \omega_2}{\omega_0} - (\alpha+1) \right] z_2. \quad (4.11)$$

These relations are equally valid for integer and non integer values of  $\beta$ . Freeman<sup>2</sup> only considered integer values. Substituting (4.4) into (2.11) and solving for the  $z_j$  gives

$$\begin{aligned}
z_1 &= -\lambda_1/\lambda_0^2 \\
z_2 &= -[\lambda_2 + (1+\lambda_0)z_1\lambda_1]/2\lambda_0^2 \\
z_3 &= -[\lambda_3 + (1+\lambda_0)z_1\lambda_2 + (1+2\lambda_0)z_2\lambda_1]/3\lambda_0^2 \\
&\vdots \qquad \qquad \qquad \vdots
\end{aligned}
\tag{4.12}$$

which may then be used in (4.11) to give relations between the  $\lambda_j$  and  $J_j$ .

These will be used later to evaluate the  $\lambda_j$  for each order of approximation.

The solution proceeds in ascending orders of approximation. The zeroth order, corresponding to the strong shock solution with  $y \rightarrow 0$ , is used in the computation of the first order solution and the first order solution is then used to compute the second and so forth. In this paper the solution will be carried only to the 2nd order.

The zeroth order approximation to the isentropic equation is

$$\frac{g_0'}{g_0} = - \left[ \frac{\lambda_0}{(\alpha+1)m} + \gamma \left( \alpha \frac{a_0'}{a_0} + \frac{\alpha_0''}{\alpha_0'} \right) \right]
\tag{4.13}$$

which Freeman has shown to have an integral

$$g_0 = K_0 / (a_0^\alpha a_0')^\gamma m^{\lambda_0/(\alpha+1)}
\tag{4.14}$$

where

$$K_0 = \frac{2\gamma}{\gamma+1} \left[ \frac{\gamma-1}{(\alpha+1)(\gamma+1)} \right]^\gamma
\tag{4.15}$$

The momentum equation in the zeroth approximation becomes

$$a''_0 = (B_0 a'_0 - C_0 a_0 - g_0 a_0^\alpha \lambda_0 / m) / A_0, \quad (4.16)$$

where

$$A_0 = (\alpha+1) \gamma [a_0^\alpha g_0 / a'_0 - (\alpha+1) m^2],$$

$$B_0 = (\alpha+1) m \gamma (\alpha + \lambda_0 / 2),$$

$$C_0 = \gamma [\lambda_0 / 2 + \alpha(\alpha+1) g_0 a_0^\alpha a'_0 / a_0^2]. \quad (4.17)$$

The first approximation to the energy integral,  $J$ , of (4.8) will be obtained by evaluating

$$J_0 = \int_0^1 \left[ \frac{\gamma}{l^2} \left( \frac{a_0 - (\alpha+1) m a'_0}{\alpha+1} \right)^2 + \frac{g_0 a_0^\alpha a'_0}{\gamma-1} \right] dm \quad (4.18)$$

along with integration of (4.16) from the shock front to the mass origin.

(Note that Freeman's forms of this and higher order integrals are only correct for  $\alpha = 1$ .) The first term of this expression is a measure of the kinetic energy behind the shock and the second term is proportional to the internal energy so these two factors can easily be accumulated separately. The integration of  $a_0$  is initiated with the boundary conditions (4.9). The values of  $a_0(m)$ ,  $a'_0(m)$ ,  $g_0(m)$  and  $g'_0(m)$  may be stored for use in the first order solution or, more conveniently, these integrations can be performed simultaneously with those for the higher order solutions.

In the zeroth order equation  $\lambda_0$  appears as a known parameter obtained from the similarity solution. In the higher order equations the  $\lambda_j$ 's appear as unknown parameters. Fortunately, the equations are linear in  $\lambda_j$  and of course the perturbation equations are linear differential equations so it follows that

superposition of solutions is valid. This property will allow evaluation of the  $\lambda_j$ 's after the equations have been integrated.

In each higher order approximation the  $g_j'$  term in the momentum equation may be eliminated with the isentropic equation and its integral,  $g_j$ . The integrals have been obtained through third order by Freeman. The momentum equation then gives higher order perturbation equations of the form

$$a_j'' = (B_j a_j' + C_j a_j + D_j + \lambda_j E_j) / A_0 \quad (4.19)$$

in which the coefficients  $B_j$  through  $E_j$  are functions only of known quantities from lower order solutions. It follows that  $a_j$  can be expressed as the linear combination

$$a_j = a_{j1} + \lambda_j a_{j2} \quad (4.20)$$

so that (4.19) gives two equations

$$\begin{aligned} a_{j1}'' &= (B_j a_{j1}' + C_j a_{j1} + D_j) / A_0 , \\ a_{j2}'' &= (B_j a_{j2}' + C_j a_{j2} + E_j) / A_0 . \end{aligned} \quad (4.21)$$

It is convenient to let the non-zero boundary condition of (4.2) be satisfied by  $a_{j1}$  so the remaining perturbations are zero at the shock. Note that the denominator,  $A_0$ , is the same for all orders of approximation. This term goes to zero at  $m = 0$  when  $\beta = 0$  causing computational difficulties which will be discussed later.

It will be evident upon substitution of  $a_j$  into the isentropic equation that  $g_j$  must be of the form

$$g_j = g_{j1} + \lambda_j g_{j2} . \quad (4.22)$$

Finally substituting  $a_j$  and  $g_j$  into the energy integral will show  $J_j$  to be of the form

$$J_j = J_{j1} + \lambda_j J_{j2} = \int_0^1 (J'_{j1} + \lambda_j J'_{j2}) dm \quad (4.23)$$

where the terms  $J_{j1}$  and  $J_{j2}$  are to be accumulated simultaneously with integration of (4.21). When  $J_{j1}$  and  $J_{j2}$  have thus been evaluated  $\lambda_j$  can be determined. After using (4.12) in (4.11) to eliminate  $z_j$  in favor of  $\lambda_j$ , (4.23) is substituted in to the left hand side of (4.11) and the result is then solved for  $\lambda_j$ . The first two of these coefficients are

$$\lambda_1 = \frac{b - J_{11}}{J_{12} + J_0[\omega_1\beta/\omega_0 - (\alpha+1)]/\lambda_0^2} \quad (4.24)$$

and

$$\lambda_2 = \frac{J_0 \lambda_1^2 G - 2\lambda_0^2 J_{21}}{J_0 H - 2\lambda_0^2 J_{22}} \quad (4.25)$$

where

$$\begin{aligned} G &= \beta(\beta-1) \omega_1^2/\omega_0^2 + (\alpha+1)(\alpha+1-\lambda_0-2\beta\omega_1/\omega_0) \\ &\quad + (1+\lambda_0) \beta \omega_2/\omega_0 \\ H &= \beta(\omega_2/\omega_0) - (\alpha+1) \end{aligned} \quad (4.26)$$

The  $\omega_j$  are obtained from (4.7). Expressions for the coefficients  $A_j$  through  $E_j$ ,  $J'_{j1}$  and  $J'_{j2}$  are listed in the Appendix.

Freeman has shown that given approximations through the  $k$ 'th order with  $k \geq 2$ , it is possible to obtain an excellent approximation to the shock position  $R(t)$  as follows. Truncate the  $\lambda$  series at the  $k+2$  term and evaluate the

last two  $\lambda_j$  in terms of those preceding and known boundaries of the  $\lambda$  vs  $y$  curve at  $y = 1$ . Thus

$$\lambda(1) = \lambda_0 + \lambda_1 + \dots + \lambda_k + \lambda_{k+1} + \lambda_{k+2} = 0 \quad (4.27)$$

$$\begin{aligned} d\lambda(1)/dy &= \lambda_1 + 2\lambda_2 + \dots + k\lambda_k + (k+1)\lambda_{k+1} + (k+2)\lambda_{k+2} \\ &= (2+\alpha)/4 \end{aligned} \quad (4.28)$$

The higher order  $\lambda$  terms in (4.12) are then zero and all the  $z_j$  can be expressed in terms of  $\lambda_0$  through  $\lambda_{k+2}$ . If  $k = 2$  the general expression for  $z_j$  when  $j \geq 5$  is

$$\begin{aligned} z_j = - & \left( [1+(j-4)\lambda_0]\lambda_4 z_{j-4} + [1+(j-3)\lambda_0]\lambda_3 z_{j-3} \right. \\ & \left. + [1+(j-2)\lambda_0]\lambda_2 z_{j-2} + [1+(j-1)\lambda_0]\lambda_1 z_{j-1} \right) / j\lambda_0^2 \end{aligned} \quad (4.29)$$

Using this and (4.12) in (4.4) and (4.6) then gives  $z(\omega)$  or  $R(t)$  for all values of  $y$ .

It was found that this procedure works very well for  $\beta = 0$ , but when  $\beta$  approaches  $\alpha + 1$  where  $\lambda \equiv 0$ , satisfaction of the final slope condition (4.28) with a limited number of terms causes a false hump in the  $\lambda$ - $y$  curve near  $y = 1$ . The procedure was therefore modified through multiplying  $\lambda_{k+2}$  as obtained by simultaneous solution of (4.27) and (4.28) by the factor  $[1-\beta/(\alpha+1)]$  and solving (4.27) for  $\lambda_{k+1}$  once again. Thus the need to meet the final slope conditions is progressively eliminated as  $\beta$  approaches  $\alpha + 1$  to give more realistic  $\lambda$ - $y$  curves.



5. EXTRAPOLATION TO  $m = 0$ .

When  $\beta = 0$  as it does in the constant energy blast wave, integration of (4.16) will show that  $a'_0 \rightarrow \infty$  and  $a_0 \rightarrow 0$  as  $m \rightarrow 0$  so it follows from (4.17) that  $A_0 \rightarrow 0$ . This latter term appears as the denominator of (4.21) so it may be anticipated that computational difficulties will be encountered near the mass origin for all orders of approximation. The problem is further compounded in evaluation of the energy integrals which contain terms proportional to  $a'_0$  and accumulate rapidly near  $m = 0$ . For example if  $\gamma = 1.1$  and  $\alpha = 1$ , sixty percent of the true value of  $J_0$  is accumulated in the last one percent of mass variation. Numerical integration all the way to the origin is clearly impossible yet it is mandatory that accurate values of  $J_j$  be obtained else the next higher order approximation be seriously in error.

Freeman<sup>2</sup> mentioned this problem and suggested an "appropriate approximation formula" but gave no details. Similar numerical problems arising in the Eulerian formation of the problem have been noted by Sakurai<sup>1</sup> and Bach and Lee<sup>4</sup>. The procedure outlined here was developed by the author and is based upon the fact that in a region close to the mass origin the pressure term,  $g_0$ , can be taken to be constant to a very high degree of approximation. Although the procedure is only necessary when  $\beta$  is close to zero, it is still valid for larger values of  $\beta$  so it can be incorporated into a computer program valid for all values of  $\beta$ .

Consider the integrand of (4.18) in which the first term is related to the kinetic energy and the second to the internal energy.

$$J'_0 = \frac{\gamma}{2(\alpha+1)} (a_0 - (\alpha+1)ma'_0)^2 - \frac{g_0 a_0^\alpha a'_0}{\gamma-1} \quad (5.1)$$

In the region near the origin, say  $m < 10^{-3}$ , the density is very low so it may be anticipated - and verified by numerical experiment - that the first

term is much smaller than the second. Furthermore it has been observed from numerical integrations that the product  $ma'_0$  approaches zero at nearly the same rate as  $a_0$  so that this first term is nearly constant. These numerical integrations also showed  $g_0$  to be constant to about four significant figures in this region. It follows that taking these factors constant over an interval of  $\Delta m \leq 10^{-3}$  will introduce no significant error in the computation of  $J_0$ .

The major contributing factor to the integral is then  $a_0^\alpha a'_0$  which by use of (4.14) can be expressed in terms of  $m$  as

$$a_0^\alpha a'_0 = (K_0/g_0)^{1/\gamma} m^{-\lambda_0/\gamma(\alpha+1)} \quad (5.2)$$

which can be integrated analytically if  $g_0$  is taken to be constant.

The procedure then is to integrate numerically from  $m = 1$  to  $m = \delta$  where  $0 < \delta \leq 10^{-3}$  and add a correction term obtained by analytical integration from 0 to  $\delta$ , i.e.,

$$\Delta J_0 = \frac{\gamma\delta}{2(\alpha+1)} (a_0 - (\alpha+1)\delta a'_0)^2 + \frac{g_0}{\gamma-1} \left( \frac{K_0}{g_0} \right)^{1/\gamma} \left[ \frac{\delta^{1-\lambda_0/\gamma(\alpha+1)}}{1-\lambda_0/\gamma(\alpha+1)} \right] \quad (5.3)$$

where  $a_0$  and  $a'_0$  are evaluated at  $m = \delta$ .

Similar considerations apply to the higher order approximations to  $J$ . In each case the kinetic energy term in the integrand can be taken as constant over the last integration interval while the internal energy term can be expressed in terms of  $a_0^\alpha a'_0$ ,  $g_0$  and essentially constant ratios such as  $a_j/a_0$ ,  $a'_j/a'_0$ , etc. This method has been checked by letting  $\delta$  take on values from  $10^{-3}$  to  $10^{-6}$  and noting that all give the same final values for each  $J_j$ . A value of  $\delta = 10^{-5}$  was used in the computations leading to the results reported in the next section. Formulas for the correction term  $\Delta J_{11}$ ,  $\Delta J_{12}$  etc. are given in the appendix.

## 6. RESULTS

The equations outlined in Sections 3, 4 and the Appendix have been numerically integrated with a fourth order Runge-Kutta algorithm in double precision and extrapolated to  $m = 0$  as discussed in Section 3. The procedure has been carried out to the second order in the expansion variable  $y$  (some authors<sup>1,2,4</sup> prefer "third approximation") for plane, cylindrical and spherical blast waves, i.e., for  $\alpha = 0, 1, 2$ . The range  $0 \leq \beta < \alpha + 1$  (above which the zeroth order similarity solution ceases to exist<sup>6</sup>) was covered for  $\gamma = 1.1$  and  $1.4$ . The solution for the case,  $\beta = \alpha + 1$ , which corresponds to the well known self similar solution for which  $\lambda = 0$  and  $R = Kt$ , is computationally unobtainable because of a zero divisor problems evident in equation 3.7. However, solutions for  $\beta$  very close to this value (within .01) were obtained easily. Solutions have also been obtained for other typical values of  $\gamma$  for integer values of  $\beta$ .

Tables 1 to 3 are summaries of the expansion coefficients  $\lambda_1$ ,  $\lambda_2$  and  $J_0$ ,  $J_1$ ,  $J_2$  obtained in the computation. Korobienikov and Chushkin<sup>5</sup>, Sakurai<sup>1</sup>, Bach and Lee<sup>4</sup> have all published values of  $\lambda_1$  computed in Eulerian coordinates for  $\beta = 0$ ,  $\gamma = 1.4$  which agree with those given here. (Note that Bach and Lee report values of  $\lambda_1/2$  while the others give values of  $\lambda_1/(\alpha+1)$ ). The values of  $\lambda_2$  and  $\lambda_1$  for  $\beta = 0$  and  $\gamma = 1.4$  are also in agreement to the full six significant figures quoted by Bach and Lee. The values of  $\lambda_1$  for  $\beta = 0$  and  $\gamma = 1.1$  to  $3.0$  are in agreement with those reported by Freeman, however his values of  $\lambda_1$  for  $\beta = 1$  are in error because he apparently used an incorrect value of  $\lambda_0$  to obtain them. His values of  $J_{11}$  and  $J_{12}$  are, however, correct. As a final check on numerical accuracy it is noted that the values of  $J_0$  reported to 4 significant figures by Rogers for  $\gamma = 1.2$  and  $1.4$  and various  $\beta$  agree with values in these tables.

It can be seen from the tables that the  $\lambda$  coefficients approach zero

rapidly as  $\beta$  is increased from zero. This is also shown in Figure 1. The maximum value of  $\beta$  is  $\alpha+1$  where  $\lambda = 0$  and the shock propagates with constant velocity. This drop off of the decay index implies much stronger convergence of the perturbation series as  $\beta$  increases.

Figure 2 shows typical variations of the J coefficients with  $\beta$  for  $\alpha = 2$ , and  $\gamma = 1.4$ . It is seen that  $J_2$  drops off rapidly and  $J_0$  becomes fairly constant while  $J_1$  takes on an increasing portion of the energy as  $\beta$  increases. Similar results obtain for other  $\gamma$  and  $\alpha$ .

Radial pressure, density and velocity distributions are presented in Figures 3 to 5 for  $\alpha = 2$ ,  $\gamma = 1.4$  and  $\beta = 0, 1, 2$ . The hump in the density distribution for  $y = .5$  and  $\beta = 0$  is most likely due to truncation of the expansion at the third term. This suggests an upper limit of validity for  $y = .5$ , or a shock Mach number of 1.4, for the second order expression when  $\beta = 0$ . This limit can be raised considerably as  $\beta$  increases as is evidenced by the curves for  $\beta = 1, 2$ .

As  $\beta$  is increased from zero, the constant energy case, the flow region rapidly contracts to a thin shell between the shock and the fictitious piston located at the zero mass position as is evident in Figures 4 and 5. Even when  $\beta = 0$ , over 99% of the mass is located in the outer half radius of the sphere but as noted before, over 50% of the total energy can be confined to the inner 1% of the mass because the temperature becomes extremely large in this region. As  $\beta$  approaches  $\alpha+1$  the solution approaches the self similar result for  $\lambda = 0$  and  $y = \text{constant}$ . At this limit the spherical blast wave flow field occupies a thin shell within which the velocity, pressure and density are constant. Similar results obtain for other  $\gamma$  and  $\alpha$ . In particular the profiles for  $\alpha = 1$ ,  $\beta = 1$  and  $\gamma = 1.4$  are given in Figure 6 as replacements for similar plots given by Freeman which, as noted before, are in error due to his use of

the incorrect value of  $\lambda$ .

The variation of the decay index,  $\lambda$ , and the shock position,  $z$ , with shock strength,  $y$ , is given in Figure 7 for a spherical shock with  $\gamma = 1.4$  and  $\beta = 0$ . The decay index was obtained by use of accurate values of  $\lambda_0$ ,  $\lambda_1$  and  $\lambda_2$  given in Table 2 and approximate values of  $\lambda_3$  and  $\lambda_4$  obtained by matching boundary conditions at  $y = 1$  as outlined in section 4. The shock position was obtained from (4.6) with  $z_j$  from (4.12) and enough terms of (4.28) to insure that no truncation error would occur in the sixth significant figure. These results are compared with a decay index and shock position obtained from tables of shock position and over-pressure reported by Goldstine and Von Neumann<sup>8</sup> who solved the exact partial differential equations by a numerical technique. The comparison is most favorable over the whole range of  $y$  even though the internal structure of the flow field can only be predicted to  $y \approx .5$  for  $\beta = 0$ . Of course when  $\beta$  becomes larger the internal approximations improve for larger  $y$ .

The effect of  $\beta$  on decay index and shock position is given in Figures 8 and 9 where  $\lambda$  and  $z$  are plotted against shock strength with  $\beta$  as a parameter. Note the smooth approach to  $\lambda = 0$  as  $\beta$  approaches  $\alpha+1$  in Figure 8.

It is evident in Figure 9 that a constant value of shock strength is approached in the limit  $\beta = \alpha+1$  or  $\beta = 3$  in this case. The value can easily be obtained by noting that a solution of the form  $z \sim \omega^n$  is required in which  $n = (2+\beta)/(\alpha+3) = 1$  to be consistent with the rest of the family of curves. Differentiating this relation and using (3.4), the definition of  $y$ , gives

$$dz/d\omega = z/\omega = y^{-1/2} \quad (6.1)$$

while the energy equation (2.22) gives

$$(\omega/z)^{\alpha+1} = Jy - 1/[(\alpha+1)(\gamma-1)] \quad (6.2)$$

Eliminating  $w/z$  and using the second order approximation for  $J$  consistent with the other curves then yields the following equation which can be solved for the limiting value of  $y$ .

$$y^{(\alpha+3)/2} = J_0 + \left( J_1 - 1/[(\alpha+1)(\gamma-1)] \right) y + J_2 y^2 \quad (6.3)$$

Taking  $\gamma = 1.4$ , the limits are  $y = 0.531, 0.528$  and  $0.542$  for  $\alpha = 2, 1$  and  $0$ , respectively.

The shock trajectories corresponding to Figures 8 and 9 are given in Figure 10. It is clear that there is relatively little difference in trajectories as  $\beta$  is varied. The major effect of increasing  $\beta$  is the faster decay of shock strength at low  $z$  and slower decay at large  $z$  previously shown in Figure 9. In addition there appears to be only a very weak dependence of the trajectory upon  $\gamma$  as the curves for  $\gamma = 1.1$  fall in the same narrow band indicated for  $\gamma = 1.4$ . The  $\gamma$  effect is more evident in the  $z$ - $y$  plots of Figure 11 which also indicate the effect of  $\alpha$  for  $\beta = 0.5$  in all cases.

The apportionment of energy between kinetic and internal modes is also of interest. These two contributions can easily be separated in the computation of the energy integral,  $J$ . The fraction of the total energy associated with kinetic energy is plotted in Figure 12 versus the shock strength with  $\beta$  as a parameter. These results were computed with a three term approximation of  $J$ . Note that the kinetic energy fraction increases with  $\beta$  while in all cases most of the energy soon is transformed to internal energy as the shock decays and  $y$  increases. The values obtained for  $y = 0$  are in agreement with computations made by Rogers<sup>3</sup>.

## REFERENCES

1. Sakurai, A., "Blast Wave Theory," *Basic Developments in Fluid Dynamics*, M. Holt Editor, Academic Press, New York, 1965, pp. 309-375.
2. Freeman, R. A., "Variable-energy Blast Waves," *British Journal of Applied Physics*, Vol. 1, 1968, pp. 1697-1710.
3. Rogers, M. H., "Similarity Flows Behind Strong Shock Waves," *Quarterly, Journal of Mechanics and Applied Mathematics*, Vol. 11, 1958, pp. 411-422.
4. Bach, G. G. and J. H. Lee, "Higher-Order Perturbation Solutions for Blast Waves," *AIAA Journal*, Vol. 7, 1969, pp. 742-744.
5. Korobeinkov, V. P. and P. I. Chushkin, *Zhurnal Prikladnoi Mekhanika i Tekhnika Fizika*, Vol. 4, 1963, pp. 48-57, (in Russian)
6. Lees, L. and T. Kubota, "Inviscid Hypersonic Flow Over Blunt-Nosed Slender Bodies," *Journal of The Aeronautical Sciences*, Vol. 24, 1957, pp. 195-202.
7. Dabora, E. K., "Variable Energy Blast Waves," *AIAA Journal*, Vol. 10, 1972, pp. 1384-1386.
8. Goldstine, H. and J. Von Neumann, "Blast Wave Calculations," *Communications on Pure and Applied Mathematics*, Vol. 8, 1955, pp. 327-353.
9. Taylor, G. I., "The Formation of a Blast Wave by Very Intense Explosion, I, Theoretical Discussion," *Proceedings of the Royal Society (London)*, Series A, Vol. 201, 1950, pp. 159-166.

$\beta$	$\gamma$	$J_0$	$\lambda_1$	$J_1$	$\lambda_2$	$J_2$	
0	1.1	2.80158	-4.17316	-0.84575	5.91593	4.14349	
	1.2	1.53186	-4.08477	-0.62865	5.09973	1.95302	
	1.3	1.09904	-4.01846	-0.54156	4.57118	1.25598	
	1.4	0.87708	-3.96712	-0.48974	4.20319	0.92163	
	5/3	0.59873	-3.87486	-0.40999	3.61729	0.54144	
	2	0.44810	-3.80867	-0.35333	3.24624	0.36366	
	3	0.27579	-3.72635	-0.26385	2.82464	0.19475	
	.25	0.70204	-2.65379	-0.02745	2.18103	0.57057	
	.5	1.1	0.78106	-1.79666	3.66353	1.33644	0.59187
		1.4	0.62794	-1.72133	0.22057	0.96355	0.36104
1.0	1.1	0.60523	-0.65358	4.20887	0.07644	0.15244	
	1.2	0.58859	-0.65324	1.73102	0.06742	0.14316	
	1.3	0.54713	-0.65407	0.91562	0.06269	0.13736	
	1.4	0.56127	-0.65559	0.51408	0.06044	0.13357	
	5/3	0.53222	-0.66114	0.04626	0.06044	0.12830	
	2	0.50269	-0.66886	-0.17246	0.06530	0.12565	
	3	0.43705	-0.68943	-0.35263	0.08495	0.12245	
	1.5	1.1	0.53960	-0.18017	4.45556	-0.05095	0.02116
		1.4	0.53039	-0.18812	0.69124	-0.04452	0.03804
	1.95	1.4	0.51401	-0.01130	0.80246	-0.00473	0.00116
1.99	1.4	0.51286	-0.00216	0.81088	-0.00093	-0.00091	

TABLE 1. EXPANSION COEFFICIENTS FOR CYLINDRICAL WAVE,  $\alpha = 1$

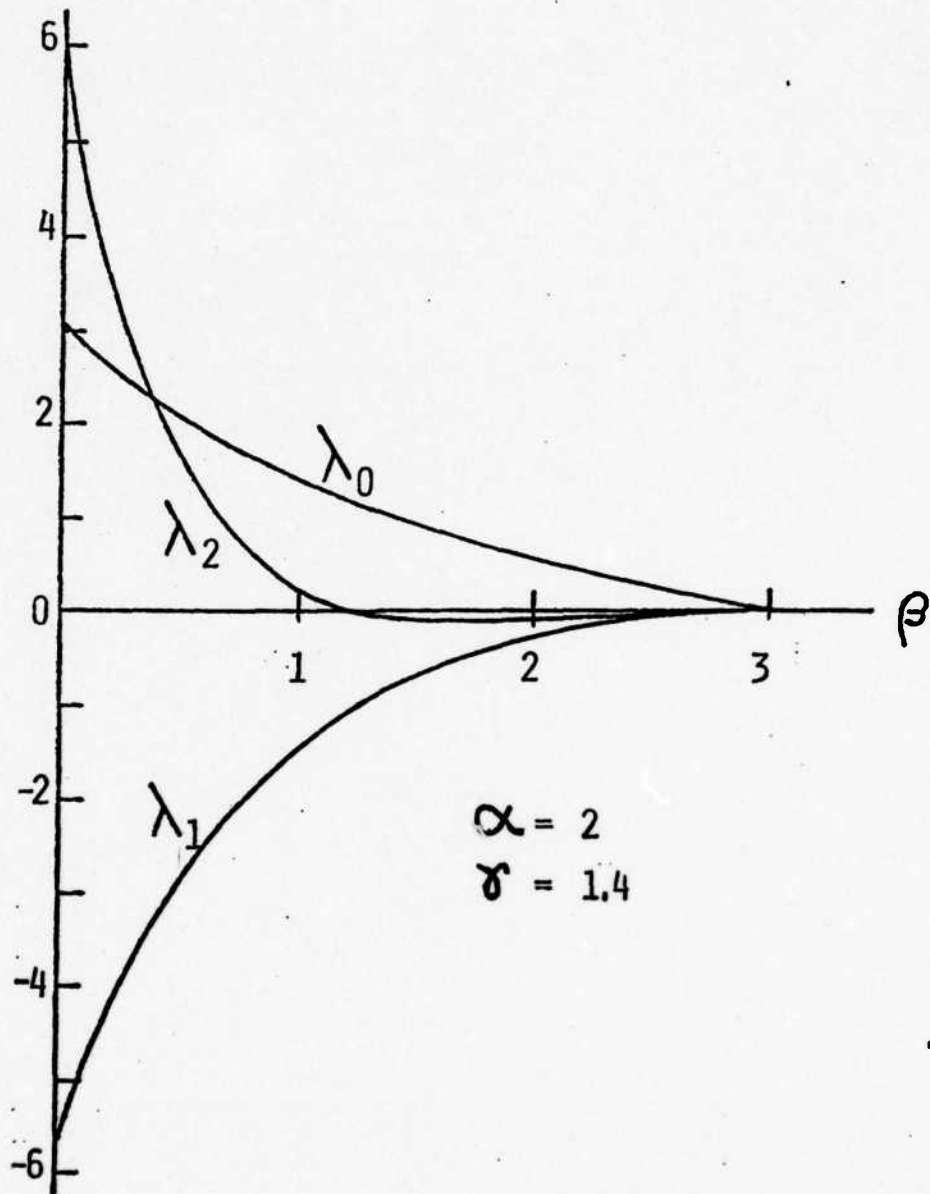


B	Y	$J_0$	$\lambda_1$	$J_1$	$\lambda_2$	$J_2$	
0 ↓	1.1	1.87082	-6.00300	-0.41019	7.75197	2.41710	
	1.2	1.02644	-5.89969	-0.35189	6.80141	1.16354	
	1.3	0.73942	-5.81883	-0.32307	6.15881	0.75899	
	1.4	0.59261	-5.75446	-0.30338	5.69937	0.56291	
	5/3	0.40915	-5.63556	-0.26860	4.94952	0.33752	
	2	0.31034	-5.54866	-0.24066	4.46598	0.23100	
	3	0.19774	-5.44223	-0.19204	3.91799	0.12912	
	.25	1.4	0.49105	-4.07792	-0.03462	3.14452	0.36095
	.5 ↓	1.1	0.57496	-3.03230	2.35264	2.33198	0.43541
		1.4	0.44325	-2.87521	0.11646	1.57621	0.23932
	1.0 ↓	1.1	0.44272	-1.43972	2.72249	0.34785	0.14331
		1.2	0.42440	-1.42411	1.08744	0.28346	0.12362
1.3		0.40974	-1.41519	0.55541	0.24441	0.11135	
1.4		0.39761	-1.41027	0.29596	0.21973	0.10322	
5/3		0.37295	-1.40748	-0.00305	0.18889	0.09144	
1.5 ↓	1.1	0.39238	-0.66360	2.88715	-0.07706	0.04510	
	1.4	0.37556	-0.66763	0.40369	-0.08871	0.04054	
2.0 ↓	1.1	0.36584	-0.27807	2.98455	-0.09847	0.00554	
	1.2	0.36489	-0.28116	1.31493	-0.09717	0.00764	
	1.3	0.36379	-0.28403	0.75685	-0.09595	0.00959	
	1.4	0.36257	-0.28669	0.47695	-0.09485	0.01137	
	5/3	0.35879	-0.29290	0.13969	-0.09243	0.01542	
2.5 ↓	1.1	0.34945	-0.08812	3.05043	-0.04453	-0.01159	
	1.4	0.35401	-0.09310	0.53054	-0.04237	-0.00205	
2.95	1.4	0.34846	-0.00629	0.56801	-0.00320	-0.00752	
2.99	1.4	0.34804	-0.00121	0.57097	-0.00062	-0.00782	

TABLE 2. EXPANSION COEFFICIENTS FOR SPHERICAL WAVE,  $\alpha = 2$

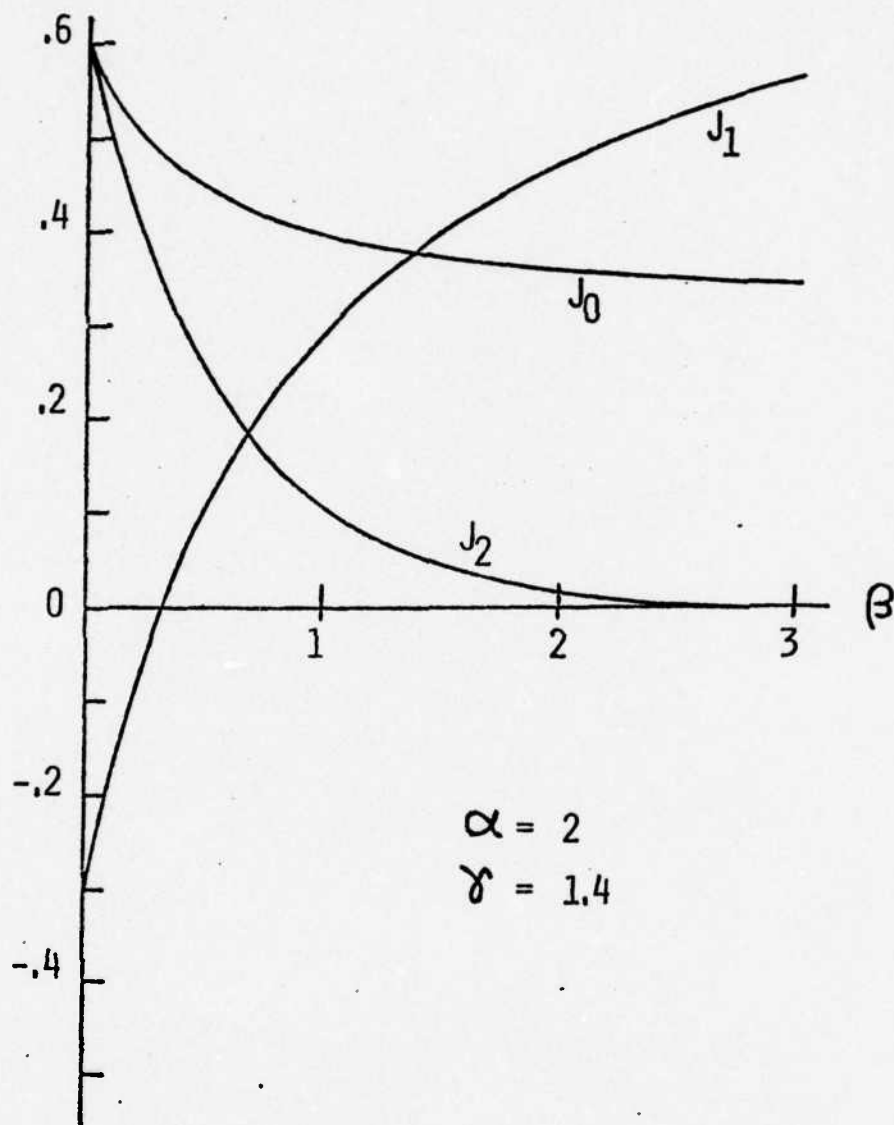
$\beta$	$\gamma$	$J_0$	$\lambda_1$	$J_1$	$\lambda_2$	$J_2$
0	1.1 1.2 1.3 1.4 5/3 2 3	5.57737 3.02287 2.14757 1.69705 1.13051 0.82425 0.47899	-2.32573 -2.24368 -2.18618 -2.14334 -2.06835 -2.01427 -1.94071	-2.97147 -1.78234 -1.36163 -1.13735 -0.83828 -0.66025 -0.42959	4.19515 3.45473 3.01386 2.72112 2.27262 1.99397 1.66803	11.69897 5.22159 3.23624 2.30893 1.28460 0.82176 0.39949
.25	1.4	1.23367	-1.20673	0.08085	1.19867	1.32576
.5	1.1 1.4	1.25640 1.08643	-0.57074 -0.56662	7.87118 0.67245	0.37492 0.34222	0.91993 0.74140
.75	1.4	1.01463	-0.19267	1.07922	0.04087	0.36683
.95	1.4	0.97925	-0.02768	1.33264	-0.00185	0.17582
.99	1.4	0.97358	-0.00517	1.37783	-0.00061	0.14599

TABLE 3. EXPANSION COEFFICIENTS FOR PLANE WAVE,  $\alpha = 0$



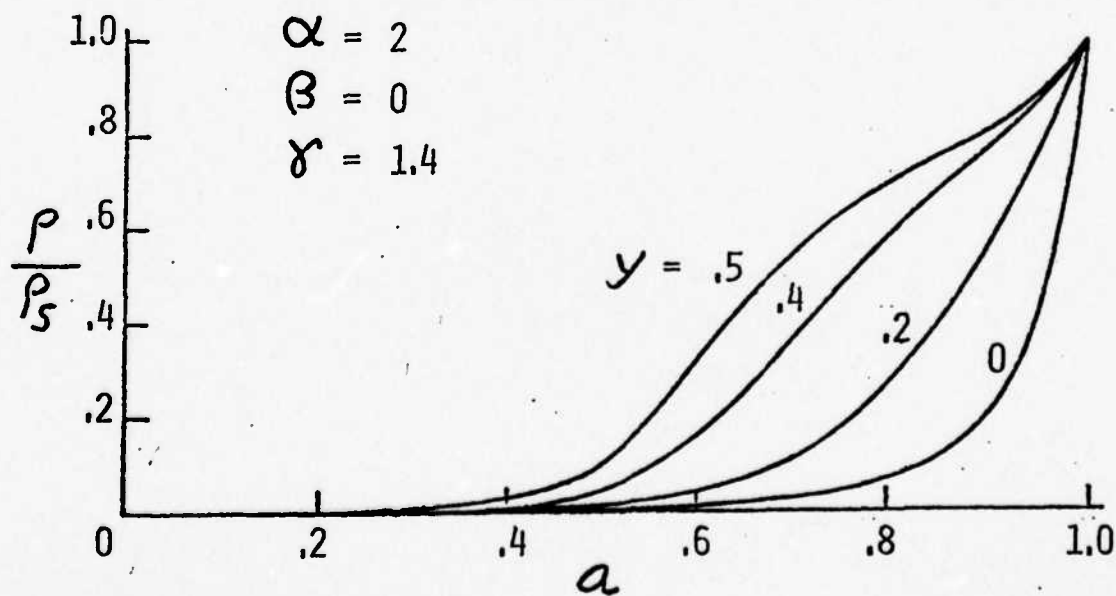
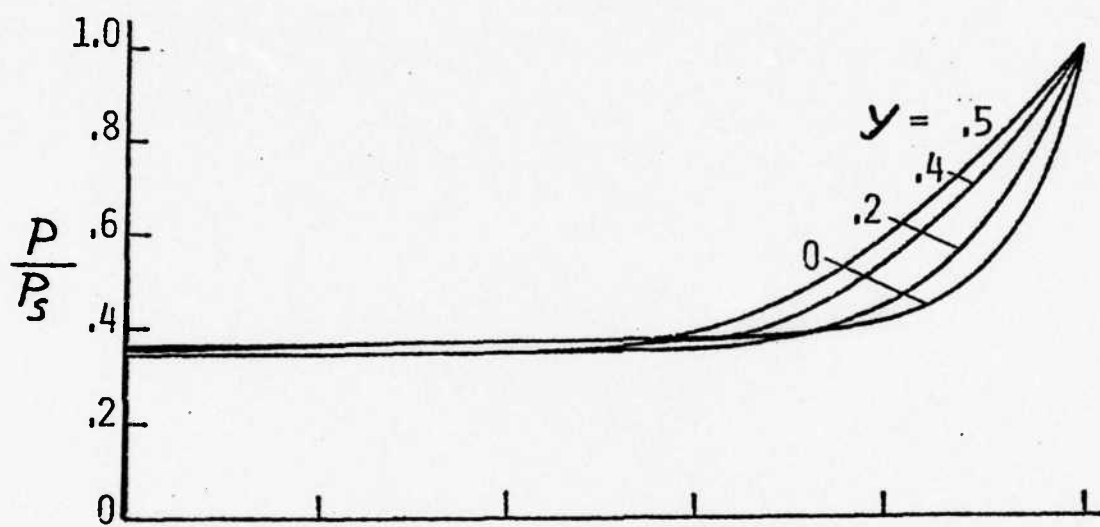
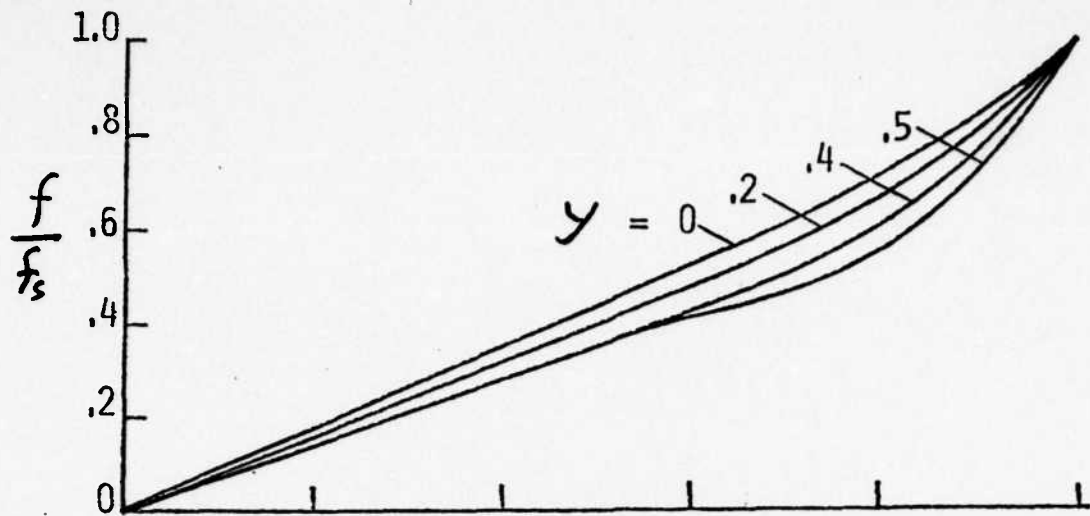
Coefficients for Decay Index Expansion as a Function of Energy Input Parameter.

Figure 1

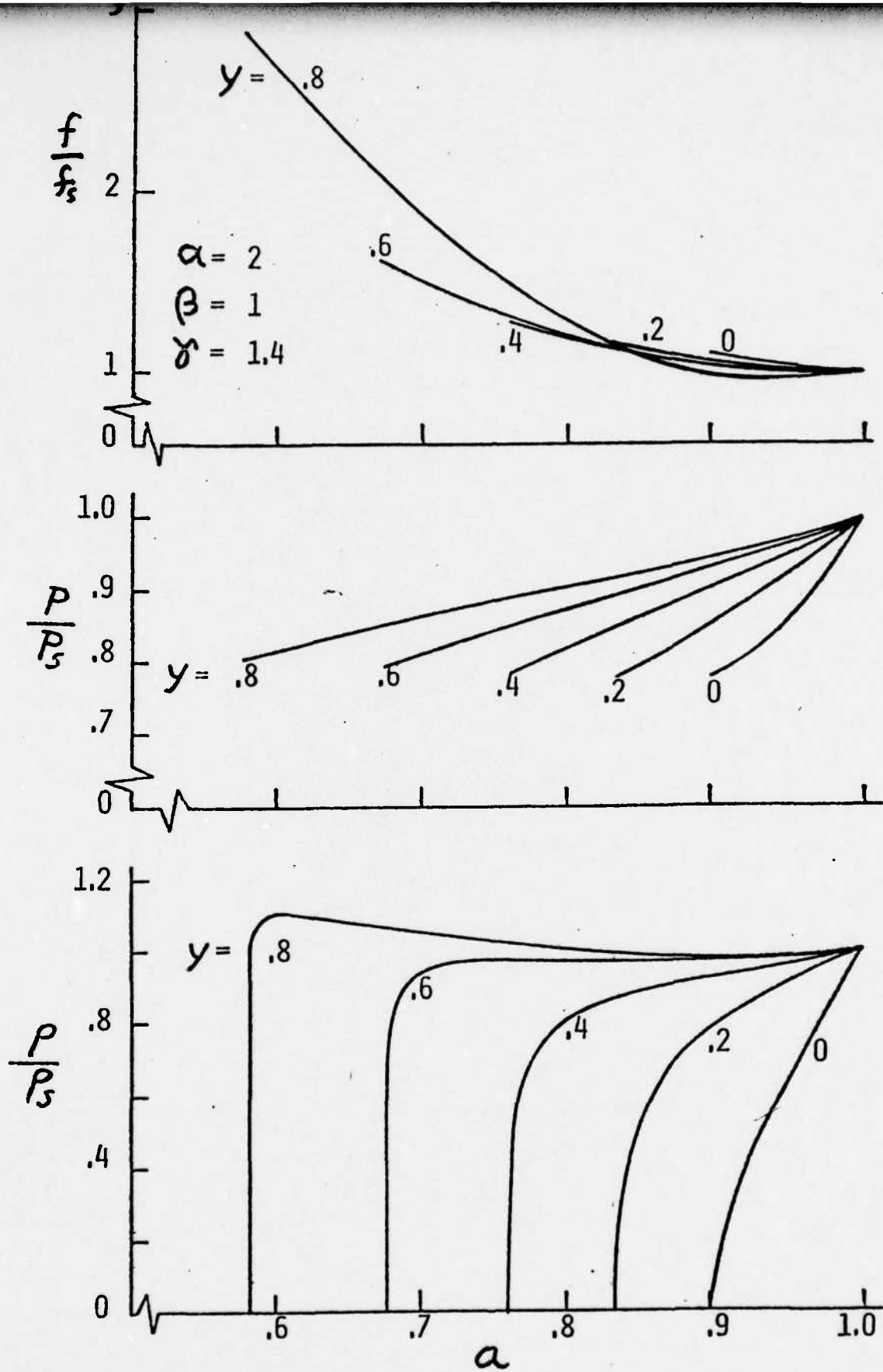


Coefficients of Energy Integral Expansion as a Function of Energy Input Parameter.

Figure 2

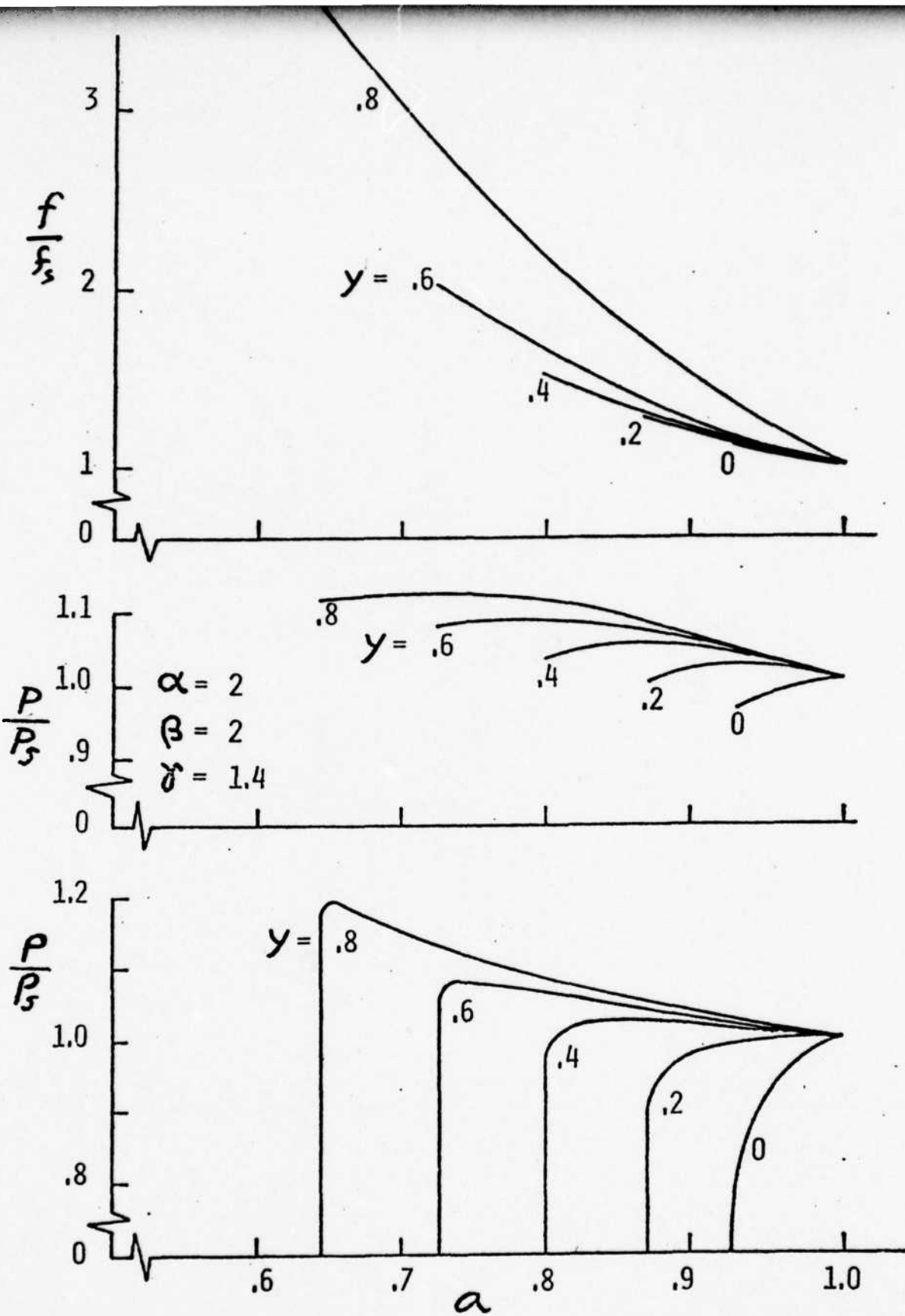


Flow Field Structure Behind Spherical Blast Wave for Instantaneous Energy Input.

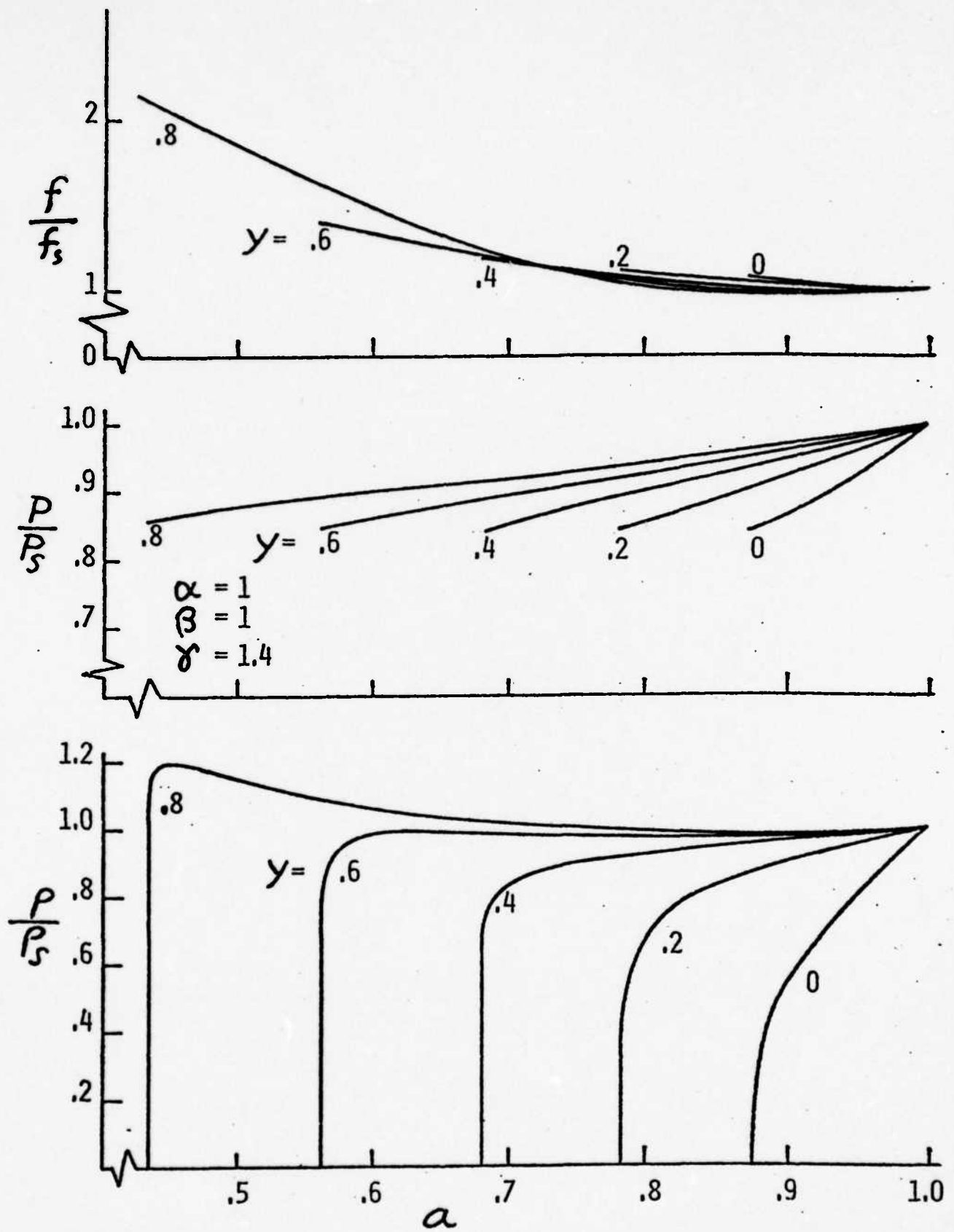


Flow Field Structure Behind Spherical Blast Wave for Constant Energy Input Rate.

Figure 4



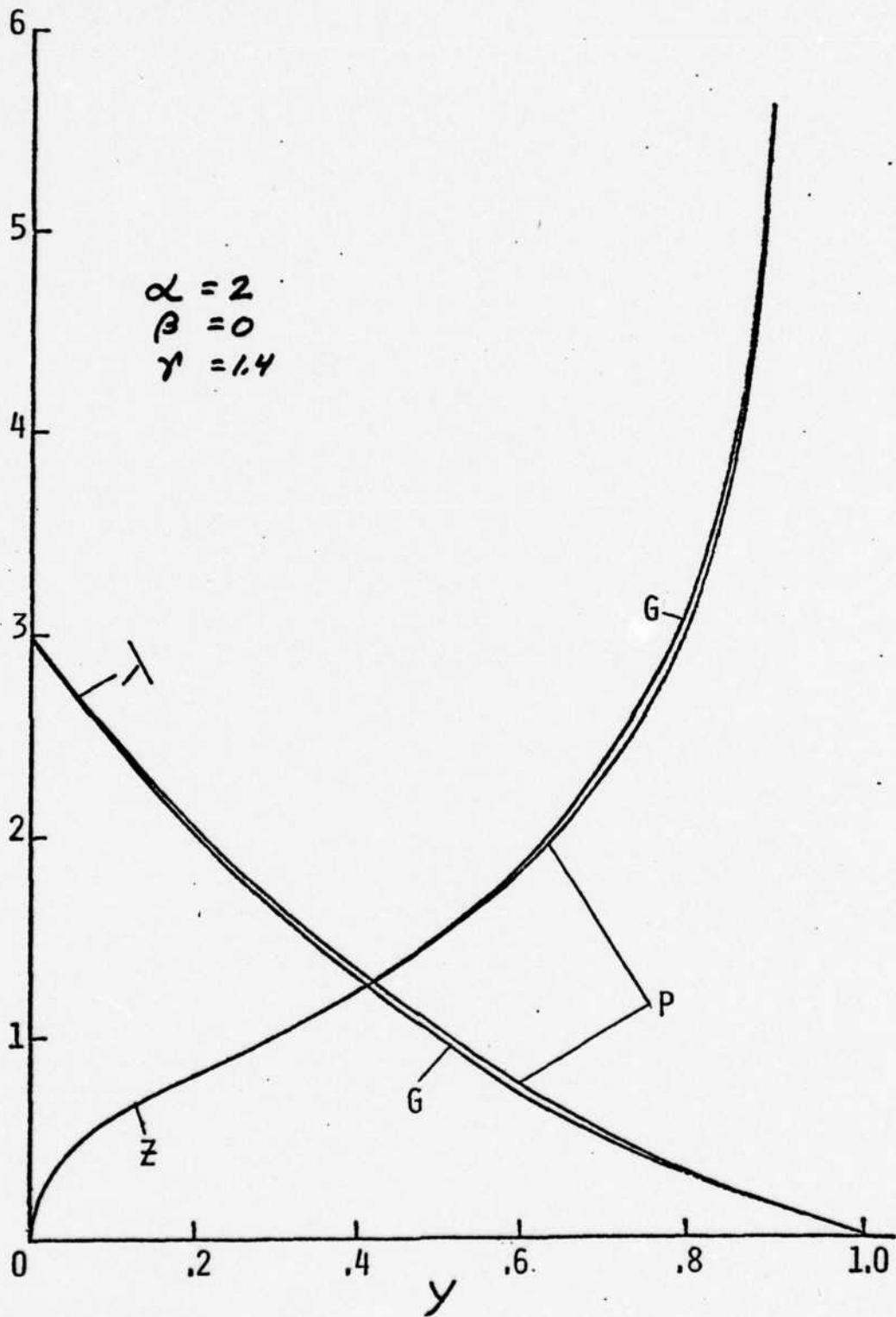
Flow Field Structure Behind Spherical Blast Wave for Linearly Increasing Energy Input Rate.



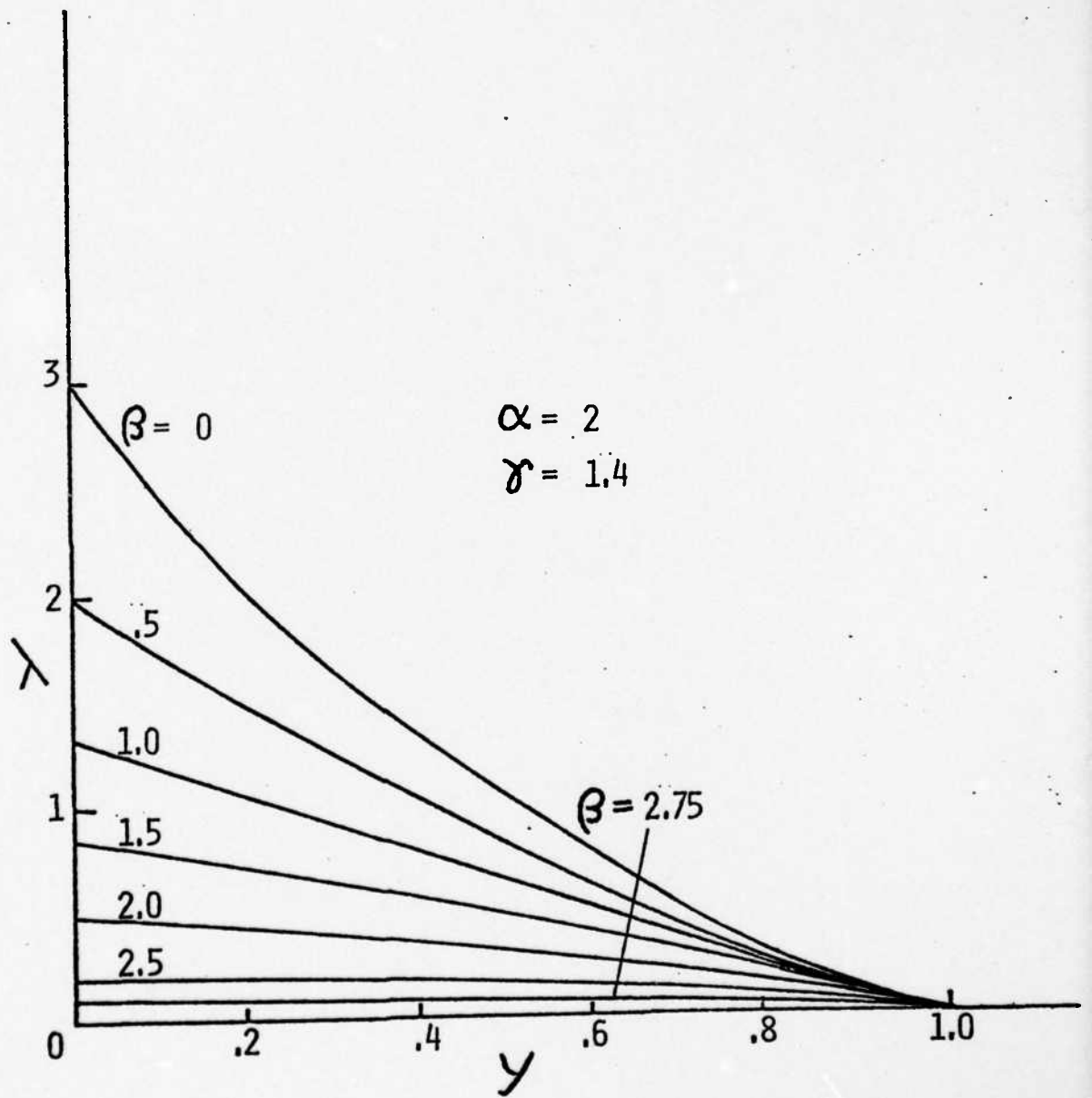
Flow Field Structure Behind Cylindrical Blast Wave for Constant Energy Input Rate.

Figure 6



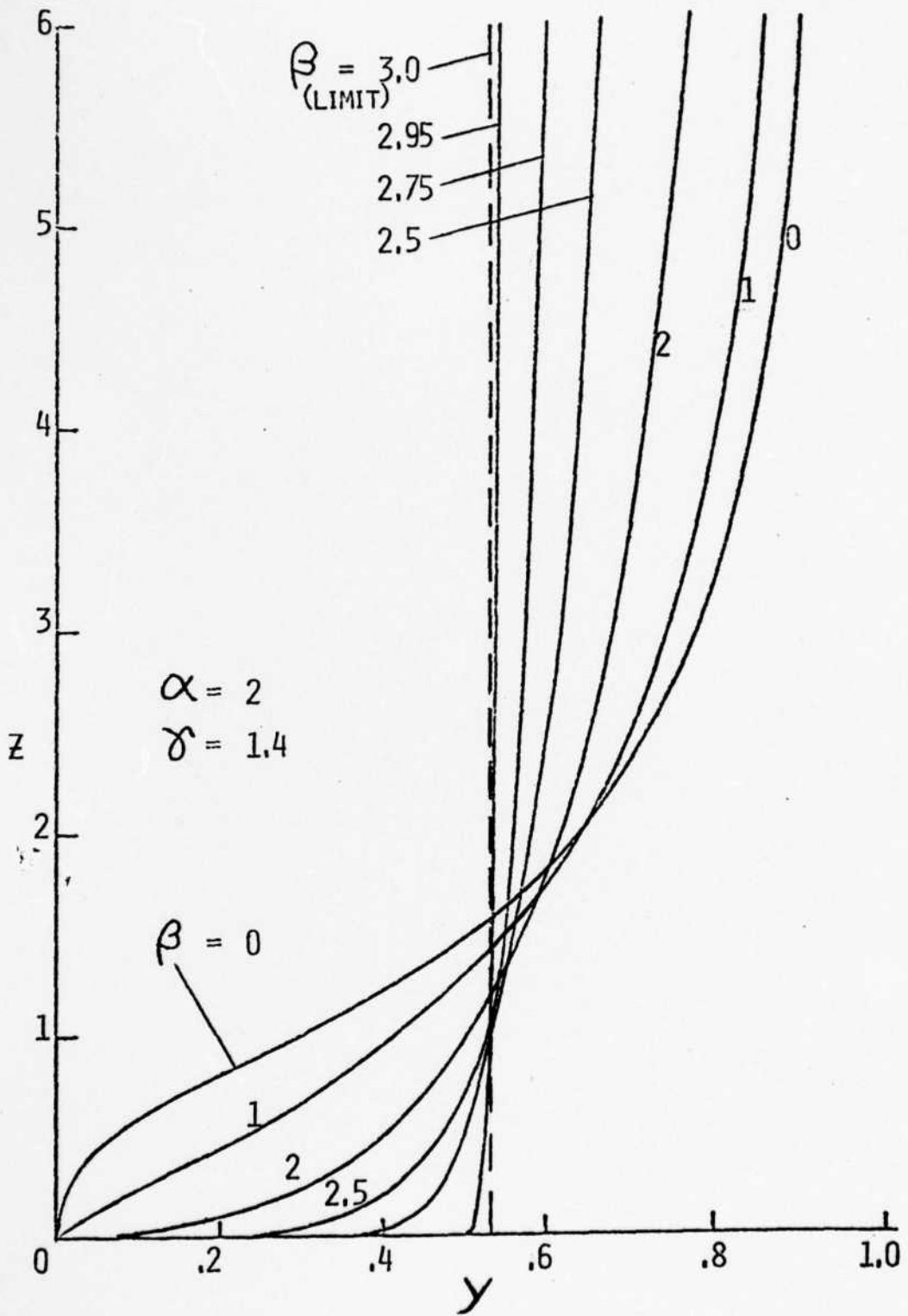


Decay Index and Shock Front Position from Second Order Perturbation Solution (P) Compared with "Exact Solution" of Goldstine and Von Neumann (G)



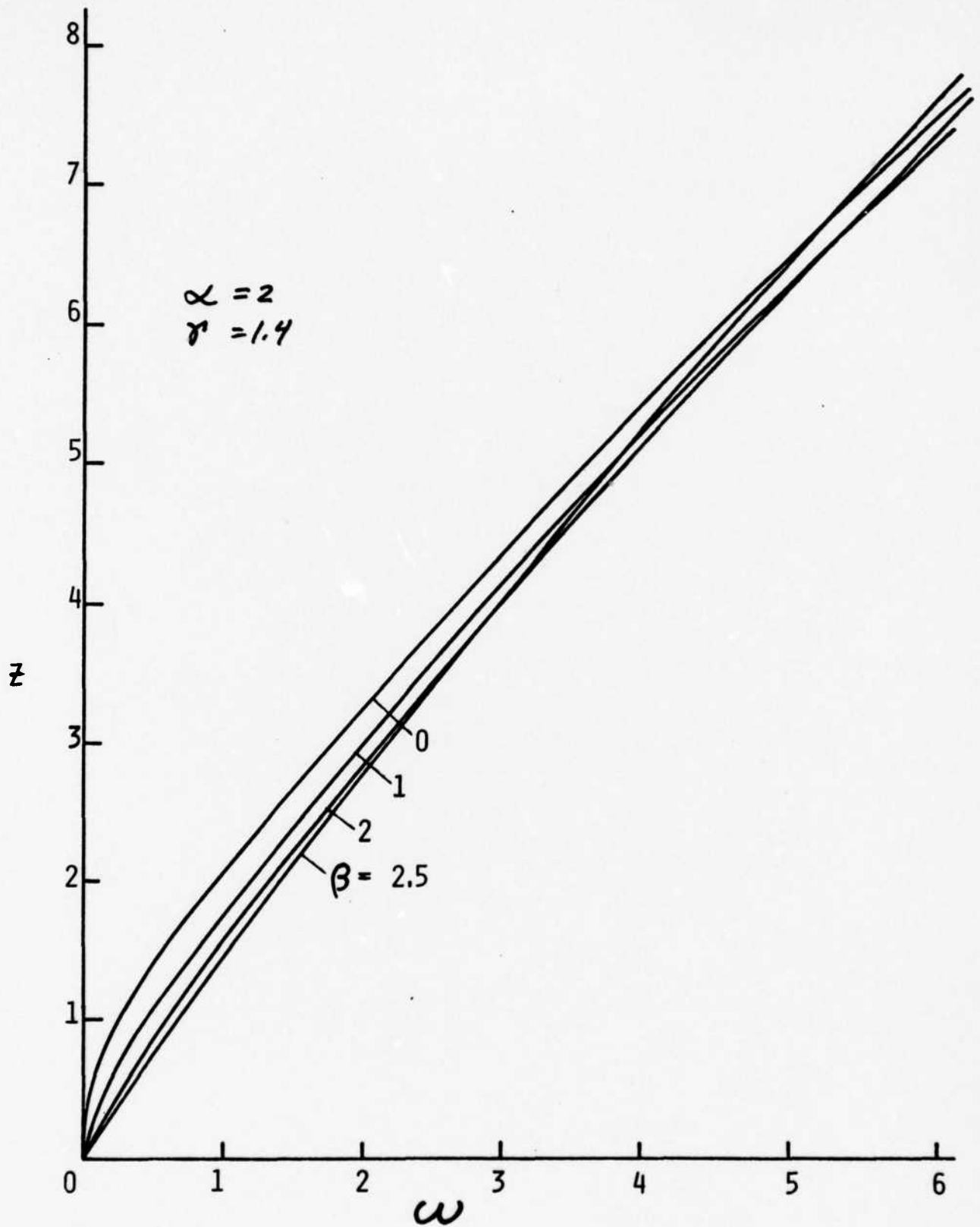
Variation of Decay Index with Shock Strength.

Figure 8



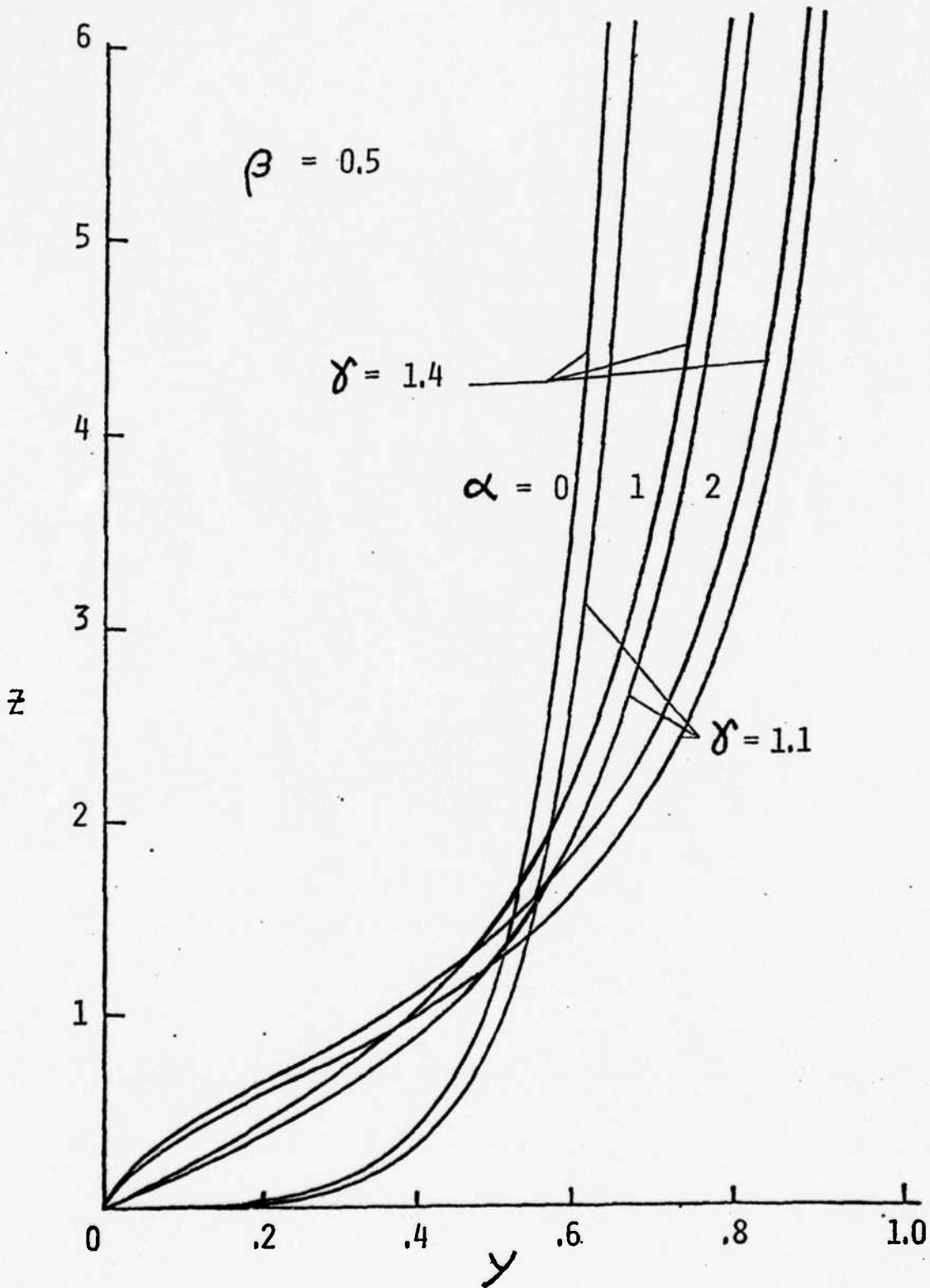
Shock Position as a Function of Shock Strength and Energy Input Parameter.

Figure 9



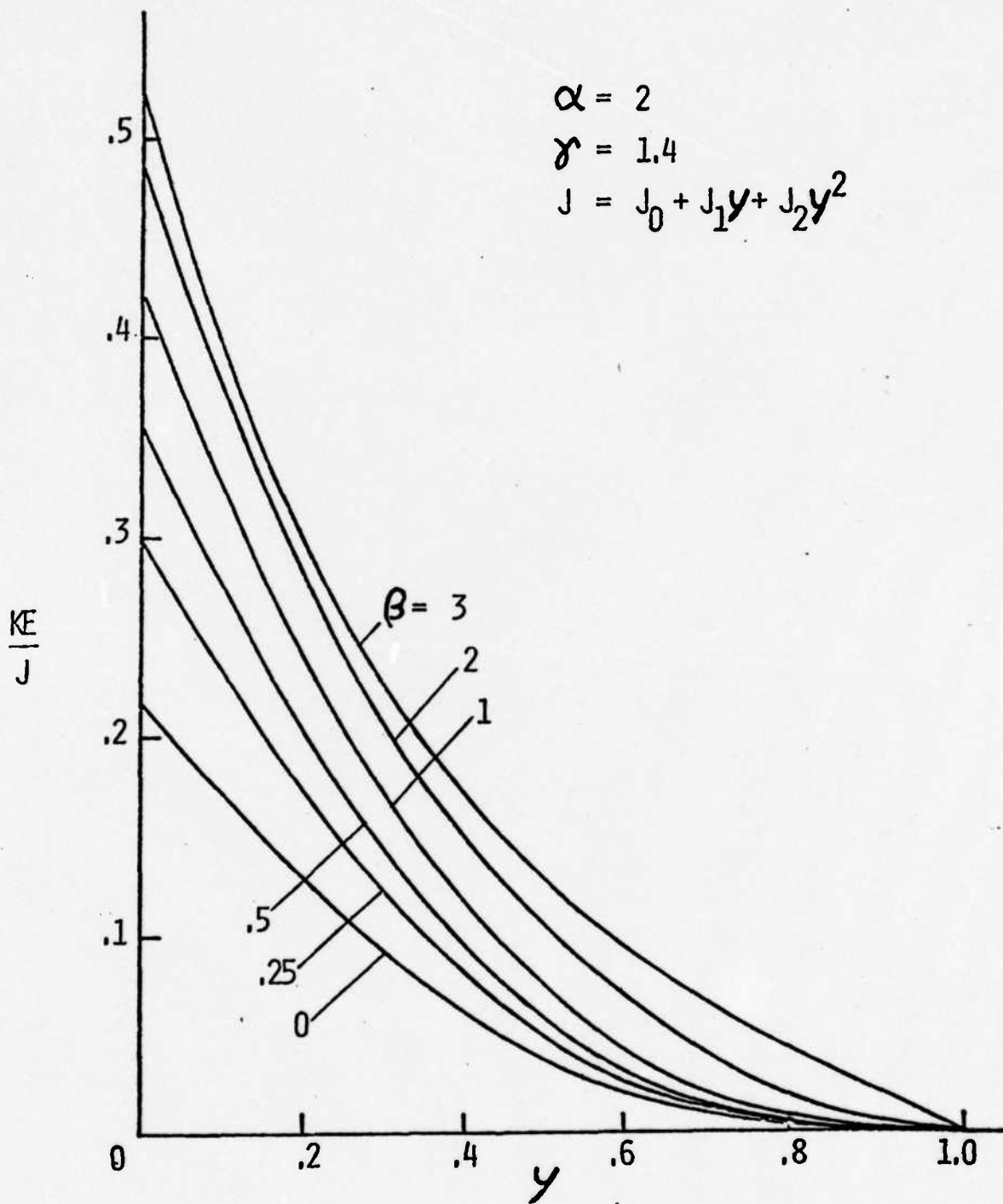
Shock Position as a Function of Time.

Figure 10



Shock Positions for Plane, Cylindrical and Spherical Blasts Compared.

Figure 11



Kinetic Energy Fraction Variation with Shock Strength and Energy Input Parameter.

Figure 12.

# BEST AVAILABLE COPY

## APPENDIX A

Summary of first and second order equations required for blast wave computation

### FIRST ORDER:

$$(A-1) \quad K_0 = \frac{2\gamma}{\gamma+1} \left[ \frac{\gamma-1}{(\alpha+1)(\gamma+1)} \right]^\gamma$$

$$(A-2) \quad K_{11} = 2\gamma/(\gamma-1) - (\gamma-1)/2\gamma$$

$$(A-3) \quad e_2 = 1 + (\gamma-1)\lambda_0/\gamma(\alpha+1)$$

$$(A-4) \quad e_1 = 1 - \lambda_0/\gamma(\alpha+1)$$

$$(A-5) \quad e_3 = 1 + (2\gamma-1)\lambda_0/\gamma(\alpha+1)$$

$$(A-6) \quad g_0 = K_0/(a_0^\alpha a_0') \gamma m \lambda_0 / (\alpha+1)$$

$$(A-7) \quad A_0 = \gamma(\alpha+1) [a_0^\alpha g_0 / a_0' - (\alpha+1)m^2]$$

$$(A-8) \quad B_0 = \gamma(\alpha+1)(2\alpha+\lambda_0)m/2$$

$$(A-9) \quad C_0 = \gamma[\alpha(\alpha+1)g_0 a_0^\alpha a_0' / a_0^2 + \lambda_0/2]$$

$$(A-10) \quad F = \gamma(a_0 - (\alpha+1)ma_0')$$

$$(A-11) \quad B_1 = B_0 + \gamma(\alpha+1) \left[ a_0^\alpha \frac{g_0 a_0''}{(a_0')^2} - \frac{g_0'}{a_0'} - \frac{g_0}{a_0} - 2m\lambda_0 \right]$$

$$(A-12) \quad C_1 = C_0 + \gamma\lambda_0^2/2 - \alpha(\alpha+1)(\gamma-1)a_0^\alpha g_0' / a_0$$

$$(A-13) \quad D_1 = K_{11} a_0^\alpha m \lambda_0 / (\alpha+1) [(\alpha+1)g_0' + g_0 \lambda_0 / m]$$

$$(A-14) \quad E_1 = [(\alpha+1)a_0^\alpha g_0' - D_1/K_{11}]/\lambda_0 - F/2$$

$$(A-15) \quad a_{11}'' = (B_1 a_{11}' + C_1 a_{11} + D_1)/A_0$$

$$(A-16) \quad a''_{12} = (B_1 a'_{12} + C_1 a_{12} + E_1) / A_0$$

$$(A-17) \quad J'_{11} = \frac{F}{(\alpha+1)} [(1+\lambda_0) a_{11} - (\alpha+1) m a'_{11}] \\ + g_0 a_0^\alpha a'_0 \left[ K_{11} \frac{m \lambda_0 / (\alpha+1)}{(\gamma-1)} - \left( \frac{a'_{11}}{a'_0} + \alpha \frac{a_{11}}{a_0} \right) \right]$$

$$(A-18) \quad J'_{12} = \frac{F}{(\alpha+1)} [(1+\lambda_0) a_{12} - (\alpha+1) m a'_{12}] \\ + g_0 a_0^\alpha a'_0 \left[ \frac{1-m \lambda_0 / (\alpha+1)}{(\gamma-1) \lambda_0} - \left( \frac{a'_{12}}{a'_0} + \alpha \frac{a_{12}}{a_0} \right) \right]$$

$$(A-19) \quad \frac{g_{11}}{g_0} = K_{11} m \lambda_0 / (\alpha+1) - \gamma \left( \frac{a'_{11}}{a'_0} + \alpha \frac{a_{11}}{a_0} \right)$$

$$(A-20) \quad \frac{g_{12}}{g_0} = \frac{1-m \lambda_0 / (\alpha+1)}{\lambda_0} - \gamma \left( \frac{a'_{12}}{a'_0} + \alpha \frac{a_{12}}{a_0} \right)$$

$$(A-21) \quad \Delta J_{11} = \int_0^\delta J'_{11} dm = \frac{F \delta}{(\alpha+1)} [(1+\lambda_0) a_{11} - (\alpha+1) \delta a'_{11}]_\delta \\ + \left[ g_0 \left( \frac{K_0}{g_0} \right)^{1/\gamma} \right]_\delta \left[ K_{11} \frac{\delta e_2}{e_2^{(\gamma-1)}} - \left( \frac{a'_{11}}{a'_0} + \alpha \frac{a_{11}}{a_0} \right) \frac{\delta e_1}{e_1} \right]$$

$$(A-22) \quad \Delta J_{12} = \int_0^\delta J'_{12} dm = \frac{F \delta}{(\alpha+1)} [(1+\lambda_0) a_{12} - (\alpha+1) \delta a'_{12}]_\delta \\ - \left[ g_0 \left( \frac{K_0}{g_0} \right)^{1/\gamma} \right]_\delta \left( \frac{\delta e_2}{e_2 \lambda_0 (\gamma-1)} + \left[ \frac{a'_{12}}{a'_0} + \alpha \frac{a_{12}}{a_0} - \frac{1}{\lambda_0 (\gamma-1)} \right]_\delta \frac{\delta e_1}{e_1} \right)$$



# BEST AVAILABLE COPY

SECOND ORDER:

$$(A-23) \quad K_1 = K_{11} - \lambda_1/\lambda_0$$

$$(A-24) \quad K_{21} = K_{11} \lambda_1/\lambda_0 - 2\gamma/(\gamma-1)^2 - (\gamma-1)^2/8\gamma^2 - \lambda_1^2/2\lambda_0^2$$

$$(A-25) \quad a_1 = a_{11} + \lambda_1 a_{12}$$

$$(A-26) \quad g_1/g_0 = g_{11}/g_0 + \lambda_1 g_{12}/g_0$$

$$(A-27) \quad \frac{g_1'}{g_0} = \frac{g_1 g_0'}{g_0^2} + \frac{K_1 \lambda_0 m^{\lambda_0}/(\alpha+1)}{(\alpha+1)m}$$

$$- \gamma \left[ \alpha \left( \frac{a_1'}{a_0} - \frac{a_1 a_0'}{a_0^2} \right) + \frac{a_1''}{a_0'} - \frac{a_1' a_0''}{(a_0')^2} \right]$$

$$(A-28) \quad G = a_1(1+\lambda_0) - (\alpha+1)ma_1'$$

$$(A-29) \quad B_2 = B_1 - 2(\alpha+1)\gamma m \lambda_0$$

$$(A-30) \quad C_2 = C_1 + (1+5\lambda_0/2)\gamma \lambda_0$$

$$(A-31) \quad D_2 = (\alpha+1)a_0^\alpha \left\{ K_{21} \lambda_0 \left[ \frac{g_0'}{\lambda_0} + \frac{2g_0}{(\alpha+1)m} \right] m^{2\lambda_0/(\alpha+1)} \right.$$

$$- K_1 \lambda_1 \left[ \frac{g_0'}{\lambda_0} + \frac{g_0}{(\alpha+1)m} \right] m^{\lambda_0/(\alpha+1)} + g_1' \left[ \frac{g_1}{g_0} + \frac{a_1}{a_0} \right]$$

$$+ \frac{g_0'}{2} \left( \gamma \left[ \alpha \frac{a_1^2}{a_0^2} + \left( \frac{a_1'}{a_0'} \right)^2 \right] - \frac{g_1^2}{g_0^2} - \frac{\lambda_1^2}{\lambda_0^2} \right)$$

$$+ \gamma g_0 \left( \frac{\alpha a_1}{a_0^3} [a_0 a_1' - a_1 a_0'] + \frac{1}{(a_0')^3} [a_0' a_1' a_1'' - (a_1')^2 a_0''] \right) \left. \right\}$$

$$+ \frac{\gamma \lambda_1}{2} [a_1(1+4\lambda_0) - 3(\alpha+1)ma_1'] + \frac{1}{2}(\alpha-1)\alpha(\alpha+1)a_1^2 g_0'$$

# BEST AVAILABLE COPY

$$(A-32) \quad E_2 = a_0^\alpha \left( \frac{(\alpha+1)g_0'}{2\lambda_0} \left[ 1 - m^{2\lambda_0/(\alpha+1)} \right] - \frac{g_0}{m} m^{2\lambda_0/(\alpha+1)} \right) - \frac{F}{2}$$

$$(A-33) \quad a_{21}'' = (B_2 a_{21}' + C_2 a_{21} + D_2) / A_0$$

$$(A-34) \quad a_{22}'' = (B_2 a_{22}' + C_2 a_{22} + E_2) / A_0$$

$$(A-35) \quad J_{21}' = \frac{1}{\alpha+1} [F(\lambda_1 a_1 + (1+2\lambda_0) a_{21} - (\alpha+1) m a_{21}') + \frac{\gamma}{2} G^2] \\ + \frac{g_0 a_0^\alpha a_0'}{\gamma-1} \left[ \frac{a_{21}'}{a_0'} + \frac{\alpha a_{21}}{a_0} + \frac{\alpha a_1}{a_0} \left( \frac{a_1'}{a_0'} + \frac{(\alpha-1) a_1}{2a_0} \right) + \frac{g_{21}}{g_0} \right. \\ \left. + \frac{g_1}{g_0} \left( \frac{a_1'}{a_0'} + \frac{\alpha a_1}{a_0} \right) \right]$$

$$(A-36) \quad J_{22}' = \frac{F'}{\alpha+1} [(1+2\lambda_0) a_{22} - (\alpha+1) m a_{22}'] \\ + \frac{g_0 a_0^\alpha a_0'}{\gamma-1} \left[ \frac{a_{22}'}{a_0'} + \frac{\alpha a_{22}}{a_0} + \frac{g_{22}}{g_0} \right]$$

$$(A-37) \quad \frac{g_{21}}{g_0} = \frac{1}{2} \left( \frac{g_1^2}{g_0^2} - \frac{\lambda_1^2}{\lambda_0^2} \right) - \gamma \left[ \alpha \left( \frac{a_{21}}{a_0} - \frac{a_1^2}{2a_0^2} \right) + \frac{a_{21}'}{a_0'} - \frac{1}{2} \left( \frac{a_1'}{a_0'} \right)^2 \right] \\ + K_{21} m^{2\lambda_0/(\alpha+1)} - \frac{K_1 \lambda_1 m^{\lambda_0/(\alpha+1)}}{\lambda_0}$$

$$(A-38) \quad \frac{g_{22}}{g_0} = \frac{1}{2\lambda_0} \left( 1 - m^{2\lambda_0/(\alpha+1)} \right) - \gamma \left( \frac{\alpha a_{22}}{a_0} + \frac{a_{22}'}{a_0'} \right)$$

# BEST AVAILABLE COPY

$$\begin{aligned}
 (A-39) \quad \Delta J_{21} &= \int_0^\delta J'_{21} dm = \frac{\delta}{\alpha+1} \left[ F(\lambda_1 a_1 + (1+2\lambda_0) a_{21} - (\alpha+1) \delta a'_{21} + \frac{\gamma}{2} G^2) \right]_\delta \\
 &+ \left[ \frac{g_0}{\gamma-1} \left( \frac{K_0}{g_0} \right)^{1/\gamma} \right]_\delta \left\{ \frac{\delta^{e_1}}{e_1} \left[ \frac{g_1}{g_0} \left( \frac{a'_1}{a_0} + \frac{\alpha a_1}{a_0} \right) + \frac{\alpha a_1}{a_0} \left( \frac{a'_1}{a_0} + \frac{(\alpha-1)a_1}{2a_0} \right) \right. \right. \\
 &+ \left. \left. \frac{1}{2} \left[ \frac{g_1^2}{g_0^2} - \frac{\lambda_1^2}{\lambda_0^2} + \gamma \left( \frac{\alpha a_1^2}{a_0^2} + \left( \frac{a'_1}{a_0} \right)^2 \right) \right] - (\gamma-1) \left( \frac{\alpha a_{21}}{a_0} + \frac{a'_{21}}{a_0} \right) \right] \right]_\delta \\
 &+ \left. \frac{K_{21} \delta^{e_3}}{e_3} - \frac{K_1 \lambda_1}{\lambda_0} \frac{\delta^{e_2}}{e_2} \right\}
 \end{aligned}$$

$$\begin{aligned}
 (A-40) \quad \Delta J_{22} &= \int_0^\delta J'_{22} dm = \frac{\delta}{\alpha+1} \left[ F(a_{22}(1+2\lambda_0) - (\alpha+1) \delta a'_{22}) \right]_\delta \\
 &+ \left[ \frac{g_0}{\gamma-1} \left( \frac{K_0}{g_0} \right)^{1/\gamma} \right]_\delta \left\{ \frac{1}{2\lambda_0} \left( \frac{\delta^{e_1}}{e_1} - \frac{\delta^{e_3}}{e_3} \right) - (\gamma-1) \left( \frac{\alpha a_{22}}{a_0} + \frac{a'_{22}}{a_0} \right) \frac{\delta^{e_1}}{e_1} \right\}
 \end{aligned}$$



# BEST AVAILABLE COPY

7A12(J) = 0.00	BLST 510
ZA21(J) = 0.00	BLST 520
ZA22(J) = 0.00	BLST 530
ZAP11(J) = Z(5)	BLST 540
ZAP12(J) = 0.00	BLST 550
ZAP21(J) = 0.00	BLST 560
ZAP22(J) = 0.00	BLST 570
ZG(J) = KN/Z(2)**GAMMA	BLST 580
ZG11(J) = ZG(J)*(AK11 - GAMMA*Z(5)/Z(2))	BLST 590
ZG12(J) = 0.00	BLST 600
ZG21(J) = 0.00	BLST 610
ZG22(J) = 0.00	BLST 620
25 WRITE(6,42) ZA(J),ZAP(J),Z(3),ZG(J),ZM(J)	BLST 630
IF(KPASS.EQ.2) GO TO 30	BLST 640
WRITE(6,43) ZA11(J),ZAP11(J),ZA12(J),ZAP12(J),Z(8),Z(9)	BLST 650
IF(KPASS.EQ.1) GO TO 50	BLST 660
30 WRITE(6,44) ZA21(J),ZAP21(J),ZA22(J),ZAP22(J),Z(14),Z(15)	BLST 670
40 FORMAT(////)	BLST 680
41 FORMAT(' ALFA =',F5.3,3X,'BETA =',F5.3,3X,'GAMMA =',F6.4,/) )	BLST 690
42 FORMAT(/,3X,'AO =',E10.4,3X,'AOPRIME =',E10.4,3X,'JO =',E11.5,3X	BLST 700
1,'GO =',E11.5,3X,'MASS =',F10.3)	BLST 710
43 FOPMAT(/,3X,'A11=',E10.4,3X,'A11PRIME=',E10.4,3X,'A12=',E10.4,3X	BLST 720
1,'A12PRIME=',E10.4,3X,'J11=',E11.5,3X,'J12=',E11.5,/) )	BLST 730
44 FOPMAT(/,3X,'A21=',E10.4,3X,'A21PRIME=',E10.4,3X,'A22=',E10.4,3X	BLST 740
1,'A22PRIME=',E10.4,3X,'J21=',E11.5,3X,'J22=',E11.5,/) )	BLST 750
45 FORMAT(/,' DJO =',F10.5,2X,'EKO =',F10.5,2X,'EFRACO =',F10.5)	BLST 760
46 FORMAT(/,' RLAM =',F10.5,2X,'K21 =',F10.5)	BLST 770
47 FOPMAT(/,' DJ11 =',F10.5,2X,'DJ12 =',F10.5,2X,'LAM1 =',F10.5,2X,	BLST 780
1'J1 =',F10.5,2X,'EK1 =',F10.5,2X,'K1 =',F10.5)	BLST 790
48 FORMAT(/,' DJ21 =',F10.5,2X,'DJ22 =',F10.5,2X,'LAM2 =',F10.5,2X,	BLST 800
1'J2 =',F10.5,2X,'EK2 =',F10.5)	BLST 810
COMMENCE INTEGRATION	BLST 820
50 DO 100 I=1,KK	BLST 830
100 CALL RUNKUT(Z,MASS,C,STEP,NV)	BLST 840
J = J-1	BLST 850
FM1 = MASS**(LAMN/ALP)	BLST 860
IF(KPASS.EQ.2) GO TO 98	BLST 870
ZM(J) = MASS	BLST 880
ZA(J) = Z(1)	BLST 890
ZAP(J) = Z(2)	BLST 900
ZG(J) = KN/((Z(1)**L*Z(2))**GAMMA*FM1)	BLST 910
ZA11(J) = Z(4)	BLST 920
ZA12(J) = Z(6)	BLST 930
ZAP11(J) = Z(5)	BLST 940
ZAP12(J) = Z(7)	BLST 950
ZG11(J) = ZG(J)*(AK11*FM1 - GAMMA*(ALFA*Z(4)/Z(1)+Z(5)/Z(2)))	BLST 960
ZG12(J) = ZG(J)*((1.00-FM1)/LAMN-GAMMA*(ALFA*Z(6)/Z(1)+Z(7)/Z(2)))	BLST 970
98 IF(KPASS.EQ.1) GO TO 99	BLST 980
ZA21(J) = Z(10)	BLST 990
ZA22(J) = Z(12)	BLST1000
ZAP21(J) = Z(11)	BLST1010
ZAP22(J) = Z(13)	BLST1020
ZG1 = ZG11(J) + LAM1*ZG12(J)	BLST1030
ZG2 = ZG1 + LAM1*Z(6)	BLST1040

# BEST AVAILABLE COPY

```

ZAP1 = Z(5) + LAM1*Z(7)
ZG21(J) = (((ZG1/ZG(J))**2-RLAM**2)/2.DO - GAMMA*(ALFA*Z(10)/Z(1)
1 + Z(11)/Z(2) - (ALFA*(ZA1/Z(1))**2 + (ZAP1/Z(2))**2)/2.DO)
2 + AK21*FM1**2 - K1*RLAM*FM1)*ZG(J)
ZG22(J) = ((1.DO-FM1**2)/2.DO/LAMN - GAMMA*(ALFA*Z(12)/Z(1) +
1 Z(13)/Z(2)))*ZG(J)
CUT DOWN STEP SIZE AS MASS APPROACHES ZERO
99 IF(J.EQ.101) STEP = STEP/10.DO
   IF(J.EQ.101) GO TO 101
   IF(J.EQ.11) GO TO 101
   IF(J.GT.2) GO TO 50
101 Z3 = -Z(3)
   WRITE(6,42) ZA(J),ZAP(J),Z3,ZG(J),ZM(J)
   IF(KPASS.EQ.2) GO TO 104
   Z8 = -Z(8)
   Z9 = -Z(9)
   WRITE(6,43) ZA11(J),ZAP11(J),ZA12(J),ZAP12(J),Z8,Z9
   IF(KPASS.EQ.1) GO TO 105
104 Z14 = -Z(14)
   Z15 = -Z(15)
   WRITE(6,44) ZA21(J),ZAP21(J),ZA22(J),ZAP22(J),Z14,Z15
105 IF(J.GT.2) GO TO 50
COMPUTE EXTRAPLATED VALUES FOR MASS = 0 WITH GO = CONSTANT
ENSTP = -.0000100
DO 202 JK=1,2
DO 200 I=1,90
200 CALL RUNKUT(Z,MASS,C,ENSTP,NV)
   FM1 = MASS**LAMN/ALP
   GN = KN/((Z(1)**L*Z(2))**GAMMA*FM1)
   Z3 = -Z(3)
   WRITE(6,42) Z(1),Z(2),Z3,GN,MASS
   IF(KPASS.EQ.2) GO TO 199
   Z8 = -Z(8)
   Z9 = -Z(9)
   WRITE(6,43) Z(4),Z(5),Z(6),Z(7),Z8,Z9
   IF(KPASS.EQ.1) GO TO 201
199 Z14 = -Z(14)
   Z15 = -Z(15)
   WRITE(6,44) Z(10),Z(11),Z(12),Z(13),Z14,Z15
201 IF(JK.EQ.2) GO TO 202
   Z25 = Z(2)
   Z45 = Z(4)
   Z55 = Z(5)
   Z65 = Z(6)
   Z75 = Z(7)
   GNS = GN
   FNSTP = ENSTP/10.DO
   IF(KPASS.EQ.1) GO TO 202
   Z105 = Z(10)
   Z115 = Z(11)
   Z125 = Z(12)
   Z135 = Z(13)
   CONTINUE
   IF(KPASS.EQ.2) GO TO 206

```

```

BLST1050
BLST1060
BLST1070
BLST1080
BLST1090
BLST1100
BLST1110
BLST1120
BLST1130
BLST1140
BLST1150
BLST1160
BLST1170
BLST1180
BLST1190
BLST1200
BLST1210
BLST1220
BLST1230
BLST1240
BLST1250
BLST1260
BLST1270
BLST1280
BLST1290
BLST1300
BLST1310
BLST1320
BLST1330
BLST1340
BLST1350
BLST1360
BLST1370
BLST1380
BLST1390
BLST1400
BLST1410
BLST1420
BLST1430
BLST1440
BLST1450
BLST1460
BLST1470
BLST1480
BLST1490
BLST1500
BLST1510
BLST1520
BLST1530
BLST1540
BLST1550
BLST1560
BLST1570
BLST1580

```

# BEST AVAILABLE COPY

<pre> AN = Z(1) ANI = AN**L ANP = Z(2) FAJ = AN - ALP*ANP*MASS GNO = (GN/GNS)*GN GN = .7D0*GN + .3D0*GNO GNKF = GN*(KN/GN)**(1.00/GAMMA)/GM FJ1 = GNKF*MASS**E1/E1 FJ2 = GNKF*MASS**E2/E2 FJ3 = GNKF*MASS**E3/E3 ANO = AN**LP - ALP*(GM/GN)*FJ1 IF(ANO.LE.1.D-13) ANO=1.D-13 ANO = ANO**(1.00/ALP) ANPO = (Z(2)/Z2S)*Z(2) DJO = GAMMA*MASS*FAJ**2/ALP/2.D0 + FJ1 AJO = DJO - Z(3) EKO = DJO - FJ1 - Z(10) EFRACO = EKO/AJO AMASS = 0.D0 WRITE(6,42) ANO,ANPO,AJO,GNO,AMASS WRITE(6,45) DJO,EKO,EFRACO A11 = Z(4) AP11 = Z(5) A12 = Z(6) AP12 = Z(7) A110 = (A11/Z4S)*A11 A120 = (A12/Z6S)*A12 AP110 = (AP11/Z5S)*AP11 AP120 = (AP12/Z7S)*AP12 G11 = GN*(AK11*FM1 - GAMMA*(ALFA*Z(4)/Z(1)+Z(5)/Z(2))) G12 = GN*((1.00-FM1)/LAMN-GAMMA*(ALFA*Z(6)/Z(1)+Z(7)/Z(2))) FK11 = GAMMA*MASS*FAJ*(LAMP1*A11/ALP - MASS*AP11) EK12 = GAMMA*MASS*FAJ*(LAMP1*A12/ALP - MASS*AP12) DJ11 = EK11 + AK11*FJ2 -GM*(ALFA*A11/AN+AP11/ANP)*FJ1 DJ12 = EK12 + (FJ1-FJ2)/LAMN - GM*(ALFA*A12/AN+AP12/ANP)*FJ1 EK11 = EK11 - Z(11) EK12 = EK12 - Z(12) AZ8 = DJ11 - Z(8) AZ9 = DJ12 - Z(9) WRITE(6,43) A110,AP110,A120,AP120,AZ8,AZ9 ZM(1) = MASS ZA(1) = AN ZAP(1) = ANP ZG(1) = GN ZA11(1) = A11 ZA12(1) = A12 ZAP11(1) = AP11 ZAP12(1) = AP12 ZG11(1) = G11 ZG12(1) = G12 IF(KPASS.EQ.1) GO TO 210 706 WRITE(6,42) ANO,ANPO,AJO,GNO,AMASS A1 = A11 + LAM1*A12 AP1 = AP11 + LAM1*AP12                 </pre>	<pre> BLST1590 BLST1600 BLST1610 BLST1620 BLST1630 BLST1640 BLST1650 BLST1660 BLST1670 BLST1680 BLST1690 BLST1700 BLST1710 BLST1720 BLST1730 BLST1740 BLST1750 BLST1760 BLST1770 BLST1780 BLST1790 BLST1800 BLST1810 BLST1820 BLST1830 BLST1840 BLST1850 BLST1860 BLST1870 BLST1880 BLST1890 BLST1900 BLST1910 BLST1920 BLST1930 BLST1940 BLST1950 BLST1960 BLST1970 BLST1980 BLST1990 BLST2000 BLST2010 BLST2020 BLST2030 BLST2040 BLST2050 BLST2060 BLST2070 BLST2080 BLST2090 BLST2100 BLST2110 BLST2120                 </pre>
---	--

# BEST AVAILABLE COPY

A21 = Z(10)	BLST2130
A22 = Z(12)	BLST2140
AP21 = Z(11)	BLST2150
AP22 = Z(13)	BLST2160
A210 = (A21/Z10S)*A21	BLST2170
A220 = (A22/Z12S)*A22	BLST2180
AP210 = (AP21/Z11S)*AP21	BLST2190
AP220 = (AP22/Z13S)*AP22	BLST2200
G1 = G11 + LAM1*G12	BLST2210
EK21 = GAMMA*MASS*(FAJ*(A21*(LAMP1+LAMN) - ALP*MASS*AP21 + LAM1	BLST2220
1*A1) + (LAMP1*A1 - ALP*MASS*AP1)**2/2.DO)/ALP	BLST2230
DJ21 = EK21 + AK21*FJ3 - K1*RLAM*FJ2 + FJ1*((G1/GN)*(ALFA*A1/AN +	BLST2240
1 AP1/ANP) + ((G1/GN)**2 - RLAM**2 + GAMMA*(ALFA*(A1/AN)**2 + (AP1	BLST2250
2/ANP)**2))/2.DO - GM*(ALFA*A21/AN+AP21/ANP) + ALFA*(A1/AN)*((ALFA	BLST2260
3 -1.DO)*A1/AN/2.DO+AP1/ANP))	BLST2270
EK22 = GAMMA*MASS*FAJ*(A22*(LAMP1+LAMN) - ALP*MASS*AP22)/ALP	BLST2280
DJ22 = EK22 + (FJ1-FJ3)/LAMN/2.DO - GM*(ALFA*A22/AN+AP22/ANP)*FJ1	BLST2290
EK21 = EK21 - Z(8)	BLST2300
EK22 = EK22 - Z(9)	BLST2310
AZ14 = DJ21 - Z(14)	BLST2320
AZ15 = DJ22 - Z(15)	BLST2330
WRITE(6,44) A210,AP210,A220,AP220,AZ14,AZ15	BLST2340
ZA21(1) = A21	BLST2350
ZA22(1) = A22	BLST2360
ZAP21(1) = AP21	BLST2370
ZAP22(1) = AP22	BLST2380
ZG21(1) = (((G1/GN)**2 - RLAM**2)/2.DO - GAMMA*(ALFA*Z(10)/Z(1)	BLST2390
1 + Z(11)/Z(2) - (ALFA*(A1/Z(1))**2 + (AP1/Z(2))**2)/2.DO)	BLST2400
2 + AK21*FM1**2 - K1*RLAM*FM1)*GN	BLST2410
ZG22(1) = ((1.00-FM1**2)/2.DO/LAMN - GAMMA*(ALFA*Z(12)/Z(1) +	BLST2420
1 Z(13)/Z(2)))*GN	BLST2430
IF(KPASS.EQ.2) GO TO 220	BLST2440
COMPUTE LAMEDAS AND ENERGY INTEGRAL CONTIBUTIONS	BLST2450
210 OMEGO = 2.DO/(LAMN+2.DO)	BLST2460
OMEG1 = (2.DO*LAMN+2.DO)/(3.DO*LAMN+2.DO)	BLST2470
LAM1 = (1.DO/GM/ALP-AZ8)/(AZ9+AJO*(BETA*OMEG1/OMEGO-ALP)/LAMN2)	BLST2480
RLAM = LAM1/LAMN	BLST2490
K1 = AK11 - RLAM	BLST2500
A21 = AK11*RLAM - 2.DO/GMOG/GM - GMOG**2/8.DO - RLAM**2/2.DO	BLST2510
AJ = AZ8 + LAM1*AZ9	BLST2520
EK1 = EK11 + LAM1*EK12	BLST2530
WRITE(6,47) DJ11,DJ12,LAM1,AJ1,EK1,K1	BLST2540
WRITE(6,46) RLAM,AK21	BLST2550
NV = 15	BLST2560
KPASS = 2	BLST2570
GO TO 20	BLST2580
220 RZ1 = -LAM1/LAMN2	BLST2590
OMEG2 = (4.DO*LAMN+2.DO)/(5.DO*LAMN+2.DO)	BLST2600
SA = (BETA*OMEG2/OMEGO - ALP)/2.DO	BLST2610
SB = -AJO*SA/LAMN2	BLST2620
SA = AJO*BZ1**2*(SA*LAMP1 + BETA*(BETA-1.DO)*(OMEG1/OMEGO)**2	BLST2630
1/2.DO + ALP*((ALFA+2.DO)/2.DO - BETA*OMEG1/OMEGO))	BLST2640
LAM2 = (SA - AZ14)/(AZ15 - SB)	BLST2650
LAM4 = -(1.00-BETA/ALP)*((ALFA+2.DO)/4.DO - LAM2 - 2.DO*LAM1 -	BLST2660



# BEST AVAILABLE COPY

```

1 3.DO*LAMN)
LAM3 = -LAMN - LAM1 - LAM2 - LAM4
AJ2 = AZ14 + LAM2*AZ15
EK2 = EK21 + LAM2*EK22
WRITE(6,48) DJ21,DJ22,LAM2,AJ2,EK2
COMPUTE SHCCK TRAJECTORY
WRITE(6,40)
BZ0 = ((2.DO+BETA)/(ALF+3.DO)**BETA/AJO)**(1.DO/(ALP-BETA))
RZ(1) = BZ1
RZ(2) = -(LAM2 + LAMP1*LAM1*BZ1)/2.DO/LAMN2
RZ(3) = -(LAM3+(LAMP1+LAMN)*LAM1*BZ(2)+LAMP1*LAM2*BZ1)/3.DO/LAMN2
RZ(4) = -(LAM4+(1.DO+3.DO*LAMN)*LAM1*BZ(3)+(LAMP1+LAMN)*LAM2*BZ(2)
1+LAMP1*LAM3*BZ1)/4.DO/LAMN2
DO 221 K=5,100
AK = K
BZ(K) = -((1.DO+(AK-4.DO)*LAMN)*BZ(K-4)*LAM4 + (1.DO+(AK-3.DO)
1*LAMN)*BZ(K-3)*LAM3+(1.DO+(AK-2.DO)*LAMN)*BZ(K-2)*LAM2
2 + (1.DO+(AK-1.DO)*LAMN)*BZ(K-1)*LAM1)/LAMN2/AK
221 OM(K) = 1.DO/(1.DO+.5DO/(AK+1.DO/LAMN))
OM(1) = OMEG1
OM(2) = OMEG2
OM(3) = 1.DO/(1.DO+.5DO/(3.DO+1.DO/LAMN))
OM(4) = 1.DO/(1.DO+.5DO/(4.DO+1.DO/LAMN))
Y = 0.DO
DO 225 I=1,20
SUMZ = 0.DO
SUMO = 0.DO
DO 222 K=1,100
TERMZ = BZ(K)*Y**K
TERMO = OM(K)*TERMZ
IF(TERMO.LT.1.D-5.AND.TERMZ.LT.1.D-5) GO TO 223
SUMZ = SUMZ + TERMZ
222 SUMO = SUMO + TERMO
223 FIRST = BZ0*Y**(1.DO/LAMN)
BZS = (1.DO + SUMZ)*FIRST
OMEGA = (OMEGO + SUMO)*FIRST*DSORT(Y)
LAMDA = LAMN + LAM1*Y + LAM2*Y**2 + LAM3*Y**3 + LAM4*Y**4
AJ = AJO + AJ1*Y + AJ2*Y**2
EK = EKO + EK1*Y + EK2*Y**2
EFRAC = EK/AJ
WRITE(6,440) Y,OMEGA,BZS,AJ,EFRAC,LAMDA
225 Y = Y + .05DO
WRITE(6,442) ALFA,BETA,AJO,AJ1,AJ2,LAMN,LAM1,LAM2,LAM3,LAM4,
1 AZ8,AZ9,AZ14,AZ15,GAMMA,SAVE
COMPUTE FLOW FIELD
IF(KFIELD.EQ.0) GO TO 10
DO 350 II=1,9
Y = 0.100*(II-1)
WRITE(6,40)
LAMDA = LAMN + LAM1*Y + LAM2*Y**2 + LAM3*Y**3 + LAM4*Y**4
WRITE(6,445) Y,LAMDA
WRITE(6,446)
DO 350 KK=1,110
IF(KK.EQ.1) GO TO 302

```

BLST2670  
BLST2680  
BLST2690  
BLST2700  
BLST2710  
BLST2720  
BLST2730  
BLST2740  
BLST2750  
BLST2760  
BLST2770  
BLST2780  
BLST2790  
BLST2800  
BLST2810  
BLST2820  
BLST2830  
BLST2840  
BLST2850  
BLST2860  
BLST2870  
BLST2880  
BLST2890  
BLST2900  
BLST2910  
BLST2920  
BLST2930  
BLST2940  
BLST2950  
BLST2960  
BLST2970  
BLST2980  
BLST2990  
BLST3000  
BLST3010  
BLST3020  
BLST3030  
BLST3040  
BLST3050  
BLST3060  
BLST3070  
BLST3080  
BLST3090  
BLST3100  
BLST3110  
BLST3120  
BLST3130  
BLST3140  
BLST3150  
BLST3160  
BLST3170  
BLST3180  
BLST3190  
BLST3200

# BEST AVAILABLE COPY

```

IF(MCD((KK-1),5).NE.0.AND.KK.LT.100) GO TO 350
IF (KK.LT.92) GO TO 302
IF(KK.GT.100) GO TO 301
JJ = 101 - (KK-91)*10
GO TO 303
301 JJ = 111 - KK
GO TO 303
302 JJ = 192 - KK
303 ZA1 = ZA1(JJ) + LAM1*ZA12(JJ)
   ZA2 = ZA2(JJ) + LAM2*ZA22(JJ)
   ZAP1 = ZAP1(JJ) + LAM1*ZAP12(JJ)
   ZAP2 = ZAP2(JJ) + LAM2*ZAP22(JJ)
   ZAT = ZA(JJ) + ZA1*Y + ZA2*Y**2
   ZAPT = ZAP(JJ) + ZAP1*Y + ZAP2*Y**2
   V = ALP*ZAT**L*ZAPT
   VEL = ZAT - ALP*ZM(JJ)*ZAPT + LAMDA*Y*(ZA1+2.DO*ZA2*Y)
   ZGT = ZG(JJ) + (ZG1(JJ) + LAM1*ZG12(JJ))*Y +(ZG21(JJ)+LAM2*
1 ZG22(JJ))*Y**2
   IF(KK.GT.1) GO TO 305
   ZGTF = ZGT
   VF = V
   VELF = VEL
305 RHO = VF/V
   ZGT = ZGT/ZGTF
   VELR = VEL/VELF
   WRITE(6,448) ZM(JJ),ZAT,ZGT,RHO,VELR
350 CONTINUE
   GO TO 10
440 FORMAT(' Y =',F6.3,' OMEGA =',E11.5,' Z =',E11.5,' J =',F10.5
1,' KE/J =',F10.5,' LAMDA =',F10.5)
442 FOPMAT('/', SUMMARY',/, ALFA=',F10.5,2X,'BETA=',F10.5,2X,'JO=',
1F10.5,2X,'J1=',F10.5,2X,'J2=',F10.5,/, LAMO=',F10.5,2X,'LAM1=',
2F10.5,2X,'LAM2=',F10.5,2X,'LAM3=',F10.5,2X,'LAM4=',F10.5,/, J11='
3,F10.5,2X,'J12=',F10.5,2X,'J21=',F10.5,2X,'J22=',F10.5,/, GAMMA='
4,F10.5,2X,'STEP=',F10.5)
445 FORMAT(/, ' Y =',F5.2,2X,'LAMDA =',F10.5)
446 FORMAT(4X,15X,'MASS',13X,'RADIUS',11X,'PRESSURE',12X,'DENSITY'
1,11X,'VELOCITY',//)
448 FORMAT(4X,5F19.5)
999 STOP
   END

```

```

BLST3210
BLST3220
BLST3230
BLST3240
BLST3250
BLST3260
BLST3270
BLST3280
BLST3290
BLST3300
BLST3310
BLST3320
BLST3330
BLST3340
BLST3350
BLST3360
BLST3370
BLST3380
BLST3390
BLST3400
BLST3410
BLST3420
BLST3430
BLST3440
BLST3450
BLST3460
BLST3470
BLST3480
BLST3490
BLST3500
BLST3510
BLST3520
BLST3530
BLST3540
BLST3550
BLST3560
BLST3570
BLST3580
BLST3590
BLST3600
BLST3610

```

# BEST AVAILABLE COPY

SUBROUTINE FCT(Z,ZP,C,M)	FCT	10
IMPLICIT REAL*8 (A-H,O-Z)	FCT	20
REAL*8 LAMN,KN,M,LAM1,K1,LAMP1	FCT	30
DIMENSION Z(15),ZP(15),C(16)	FCT	40
C AND Z TRANSFERS	FCT	50
IF(M.NE.1.DO) GO TO 10	FCT	60
LAMN = C(1)	FCT	70
KN = C(2)	FCT	80
K1 = C(3)	FCT	90
ALP = C(4)	FCT	100
GAMM = C(5)	FCT	110
GMCG = C(6)	FCT	120
AK11 = C(7)	FCT	130
AK21 = C(8)	FCT	140
RLAM = C(10)	FCT	150
LAM1 = C(11)	FCT	160
ALF = C(12)	FCT	170
GAM = C(13)	FCT	180
LAMP1 = LAMN + 1.DO	FCT	190
L = ALF + .0100	FCT	200
10 AN = Z(1)	FCT	210
ANP = Z(2)	FCT	220
COMPUTE COMMON TERMS	FCT	230
ANL = AN**L	FCT	240
FM1 = M**((LAMN/ALP)	FCT	250
GN = KN/(ANL*ANP)**GAM/FM1	FCT	260
FAJ = AN - ALP*M*ANP	FCT	270
AA = ALP*GAM*(ANL*GN/ANP - ALP*M**2)	FCT	280
COMPUTE ZERO ORDER DERIVATIVES	FCT	290
R = ALP*GAM*(2.DO*ALF + LAMN)*M/2.DO	FCT	300
CO = GAM*(LAMN/2.DO + GN*ALF*ALP*ANL*ANP/AN**2)	FCT	310
ZP(1) = ANP	FCT	320
ZP(2) = (8*ANP - CO*AN - GN*ANL*LAMN/M)/AA	FCT	330
EKO = GAM*FAJ**2/ALP/2.DO	FCT	340
ZP(3) = EKO + GN*ANL*ANP/GAMM	FCT	350
COMPUTE FIRST ORDER DERIVATIVES	FCT	360
A11 = Z(4)	FCT	370
AP11 = Z(5)	FCT	380
A12 = Z(6)	FCT	390
AP12 = Z(7)	FCT	400
ANPP = ZP(2)	FCT	410
GNP = -GN*(LAMN/ALP/M + GAM*(ALF*ANP/AN+ANPP/ANP))	FCT	420
BB = ALP*GAM*(ANL*(GN*ANPP/ANP**2 - GNP/ANP - ALF*GN/AN)	FCT	430
1 -2.DO*LAMN*M) + R	FCT	440
CC = CO + GAM*LAMN**2/2.DO - GAMM*ALF*ALP*ANL*GNP/AN	FCT	450
DD = AK11*FM1*ANL*(GNP*ALP + GN*LAMN/M)	FCT	460
EE = (ANL*ALF*GNP - DD/AK11)/LAMN - FAJ*GAM/2.DO	FCT	470
ZP(4) = AP11	FCT	480
ZP(5) = (8R*AP11+CC*A11+DD)/AA	FCT	490
ZP(6) = AP12	FCT	500
ZP(7) = (8R*AP12+CC*A12+EE)/AA	FCT	510
IF(K1.NE.0.DO) GO TO 100	FCT	520
EK11 = GAM*FAJ*(A11*LAMP1-ALP*M*AP11)/ALP	FCT	530
EK12 = GAM*FAJ*(A12*LAMP1-ALP*M*AP12)/ALP	FCT	540

# BEST AVAILABLE COPY

ZP(8) = EK11 + GN*ANL*(AK11*ANP*FM1/GAMM-AP11-ALF*ANP*A11/AN)	FCT 550
ZP(9) = EK12 + GN*ANL*(ANP*(1.00-FM1)/GAMM/LAMN - AP12	FCT 560
1 - ALF*ANP*A12/AN)	FCT 570
ZP(10) = EKO	FCT 580
ZP(11) = EK11	FCT 590
ZP(12) = EK12	FCT 600
RETURN	FCT 610
COMPUTE SECOND ORDER DERIVATIVES	FCT 620
100 A1 = A11 + LAM1*A12	FCT 630
AP1 = AP11 + LAM1*AP12	FCT 640
APP1 = ZP(5) + LAM1*ZP(7)	FCT 650
G1 = GN*(RLAM - GAM*(ALF*A1/AN + AP1/ANP) + K1*FM1)	FCT 660
GP1 = G1*GNP/GN + GN*(K1*LAMN*FM1/M/ALP - GAM*(ALF*(AP1/AN-A1	FCT 670
1*ANP/AN**2) + (APP1/ANP-AP1*ANPP/ANP**2))	FCT 680
A21 = Z(10)	FCT 690
AP21 = Z(11)	FCT 700
A22 = Z(12)	FCT 710
AP22 = Z(13)	FCT 720
BBB = BB - 2.00*ALP*GAM*M*LAMN	FCT 730
CCC = CC + GAM*LAMN*(1.00+2.500*LAMN)	FCT 740
DDD = AK21*LAMN*FM1**2*(GNP/LAMN+2.00*GN/ALP/M) - K1*LAM1*FM1*	FCT 750
1(GNP/LAMN+GN/ALP/M) + GNP*(GAM*(ALF*(A1/AN)**2+(AP1/ANP)**2) -	FCT 760
2(G1/GN)**2-RLAM**2)/2.00+GP1*(G1/GN+ALF*A1/AN)+GAM*GN*(ALF*A1*	FCT 770
3(AN*AP1-A1*ANP)/AN**3 + (ANP*AP1*APP1-AP1**2*ANPP)/ANP**3)	FCT 780
DDD = DDD*ALP*ANL + GAM*LAM1*(A1*(1.00+4.00*LAMN) - 3.00*ALP*M*	FCT 790
1 AP1)/2.00 + ALP*ALF*(ALF-1.00)*A1**2*GNP/2.00	FCT 800
EFE = .500*ALP*(ANL*GNP*(1.00-FM1**2)/LAMN + GAM*M*ANP) -	FCT 810
1 ANL*GN*FM1**2/M - GAM*AN/2.00	FCT 820
ZP(10) = AP21	FCT 830
ZP(11) = (BBB*AP21+CCC*A21+DDD)/AA	FCT 840
ZP(12) = AP22	FCT 850
ZP(13) = (BBB*AP22+CCC*A22+EEE)/AA	FCT 860
G21 = (((G1/GN)**2-RLAM**2)/2.00 + AK21*FM1**2 - RLAM*K1*FM1	FCT 870
1 - GAM*(ALF*(A21/AN-(A1/AN)**2/2.00) + AP21/ANP - (AP1/ANP)**2	FCT 880
2/2.00))*GN	FCT 890
G22 = GN*((1.00-FM1**2)/LAMN/2.00 - GAM*(ALF*A22/AN+AP22/ANP))	FCT 900
EK21 = GAM*(FAJ*(LAM1*A1 + (LAMP1+LAMN)*A21 - ALP*M*AP21)	FCT 910
1 + (LAMP1*A1 - ALP*M*AP1)**2/2.00)/ALP	FCT 920
ZP(14) = EK21 + ANL*ANP*((ALF*A21/AN + AP21/ANP + (AP1/ANP+(ALF	FCT 930
1-1.00)*A1/AN/2.00)*ALF*A1/AN)*GN+G1*(AP1/ANP+ALF*A1/AN)+G21)/GAMM	FCT 940
EK22 = GAM*(FAJ*((LAMP1+LAMN)*A22 - ALP*M*AP22))/ALP	FCT 950
ZP(15) = EK22 + ANL*ANP*(GN*(ALF*A22/AN+AP22/ANP) + G22)/GAMM	FCT 960
ZP(8) = EK21	FCT 970
ZP(9) = EK22	FCT 980
RETURN	FCT 990
END	FCT 1000

# BEST AVAILABLE COPY

SUBROUTINE RUNKUT(Z,X,C,H,N)	RNKT 10
CONSTANT STEP, FOURTH ORDER RUNGE-KUTTA INTEGRATION ALGORITHM	RNKT 20
IMPLICIT REAL*8 (A-H,O-Z)	RNKT 30
DIMENSION Z(15),C(16),Y(15),RK1(15),RK2(15),RK3(15),RK4(15)	RNKT 40
H2 = H/2.00	RNKT 50
CALL FCT(Z,RK1,C,X)	RNKT 60
DO 10 J=1,N	RNKT 70
10 Y(J) = Z(J) + H2*RK1(J)	RNKT 80
X = X+ H2	RNKT 90
CALL FCT(Y,RK2,C,X)	RNKT 100
DO 11 J=1,N	RNKT 110
11 Y(J) = Z(J) + H2*RK2(J)	RNKT 120
CALL FCT(Y,RK3,C,X)	RNKT 130
DO 12 J=1,N	RNKT 140
12 Y(J) = Z(J) + H *RK3(J)	RNKT 150
X = X+ H2	RNKT 160
CALL FCT(Y,RK4,C,X)	RNKT 170
DO 13 J=1,N	RNKT 180
13 Z(J) = Z(J) + H*(RK1(J)+2.00*(RK2(J)+RK3(J))+RK4(J))/6.00	RNKT 190
RETURN	RNKT 200
END	RNKT 210

ATE  
LMED

— 7